Lower Passaic River

System Understanding of Sediment Transport

CONTENTS

List of Figures 2
Introduction 4
System Overview 4
    Estuarine Circulation and River Flow 5
    Sediment Transport 6
Transport Characterization 7
  Water Column 7
  Mass Balance 9
  Morphology 10
  Sediment Bed 11
Summary 13
  Data Analysis Gaps 14
References 16
Figures 17

LIST OF FIGURES

Figure 1. Map of the Lower Passaic River region (Appendix A, CCSM). 18
Figure 2. Conceptual diagram of processes related to sediment and contaminant transport. 19
Figure 3. Variation in river cross-sectional area with river mile numbered from river mile 0 at the mouth (Appendix A, CCSM). 20
Figure 4. Estuarine processes active in the Lower Passaic River, a partially mixed estuary. 21
Figure 5. Time series of combined tidal (red) and tidally filtered velocities (blue) from the LPR hydrodynamic model (HQI, 2008), in the tidal fresh region (upper panel) and the estuarine region (lower two panels). In these plots positive velocities are in the flood direction (up-river) and negative velocities are in the ebb direction (down-river). 22
Figure 6. Conceptual contribution of three forcing factors relevant to transport in the Lower Passaic River. The figure represents median flow conditions at the Dundee Dam. 23
Figure 7. Conceptual contribution of three forcing factors relevant to transport in the Lower Passaic River. The figure represents elevated flow conditions at the Dundee Dam. 24
Figure 8. Location of high tide salt front as a function of flow rate determined from the HQI hydrodynamic model (Appendix A, CCSM). 25
Figure 9. Estuarine and sediment transport processes active in the Lower Passaic River. 26
Figure 10. Longitudinal profiles of salinity and total suspended solids from Chant (2009) corresponding to 1 and 330 m^3/s river flow rates respectively. 27
Figure 11. Longitudinal profiles of TSS (top) and salinity (bottom) during low flow conditions in August 2004 from preliminary HQI hydrodynamic and sediment transport model. 28
Figure 12. Tidally averaged velocity profile during low flow conditions in August 2004 from preliminary HQI hydrodynamic and sediment transport model. The profile is located at river mile 5. Negative velocity is directed downstream. 29
Figure 13. Time series of OSI turbidity data from two moorings (top). Plots of high vs. low tide turbidity and flood vs. ebb turbidity (bottom). 30
Figure 14. Time series profiles of salinity (red lines are surface and blue lines are bottom of the water column) and TSS (solid contours) near RM 3 from Chant et al. (2009) corresponding to high and low river flow rates respectively. 31
Figure 15. Sediment transport (positive is upstream) as a function of tidal range and river discharge (flow rate) estimated from current meter and backscatter measurements near RM 3 (Chant et al., 2009). 32
Figure 16. Sediment transport (negative is upstream) estimated as a function of river flow rate near RM 3 (Chant, 2009). 33
Figure 17. Sediment balance during low and elevated river flow periods. The size of each component is relative to the contribution of each term in the balance. 34
Figure 18. Flow rate and estimated cumulative transport near RM 3 (top) and cumulative river input from the Dundee Dam and estimated transport near RM 3 (bottom) from October 1994 through September 2005. 35

Figure 19. Daily water column sediment transport (negative is upstream) as a function of flow rate at 8 river mile stations in the Lower Passaic calculated from preliminary HQI hydrodynamics and sediment transport model. 36
Figure 20. Depth of the river channel based on a 2004 bathymetric survey as well as the original dredged elevations as reported in USACE records. 37
Figure 21. Estimated depths of the river channel from Chant et al. (2009). 38
Figure 22. Shaded multibeam data and contours from the 2008 survey and an overlay of qualitatively identified morphologic regions near RM 2. 39
Figure 23. Shaded multibeam data and contours from the 2008 survey and an overlay of qualitatively identified morphologic regions near RM 4. 40
Figure 24. Shaded multibeam data and contours from the 2008 survey and an overlay of qualitatively identified morphologic regions near RM 6. 41
Figure 25. Shaded multibeam data from the 2008 survey highlighting bed features near RM 2.7 (left) and RM 8.3 (left). 42
Figure 26. Side scan bottom texture identification from RM 0-6 and 8-12. 43
Figure 27. Side scan bottom texture identification from near RM 8. 44
Figure 28. Side scan bottom texture identification and computed percent fines from the 2008 core data. 45
Figure 29. Locations of the three upper river 2005 CCSM cores. 46
Figure 30. Locations of the two lower river 2005 CCSM cores. 47
Figure 31. Profiles of Cs-137 for the 5 2005 CCSM cores with 1995 PCB profiles overlain. 48
Figure 32. Shaded multibeam data from the 2008 survey and SPI camera deposition depths with photos at RM 3.9. 49
Figure 33.Conceptual diagram of key processes during low river flow conditions. 50
Figure 34. Conceptual diagram of key processes during high river flow conditions. 51

INTRODUCTION

Historically, the Lower Passaic River (LPR) below the Dundee Dam (Figure 1) has been contaminated with a range of Contaminants of Potential Concern (COPCs). Many of these contaminants are hydrophobic and therefore strongly sorb to sediments in the system. Over time the accumulation of these contaminated sediments has resulted in a persistent COPC signal in the LPR that is of environmental concern. Generally, the hydrophobic COPCs are strongly associated with the fine sediment organic material present in the LPR. Since the most significant transport pathway for these hydrophobic COPCs is by transport of the sediments to which they are sorbed, sediment transport is a key system-wide process to understand when evaluating environmental risk and any remedial selection.

In the most basic terms, sediment transport begins with the erosion, or mobilization, of sediment from one location where there is relatively high energy (e.g. watershed, river bed) due to currents, waves, and anthropogenic activities (e.g. ship propeller scour). Once mobilized, the sediment is transported in the water column to a location where there is less energy where it deposits out of the water column and comes to rest. While mobilized, contaminated sediments not only carry the mass of contaminants sorbed to them, but also release contaminated pore water from the sediment bed where they are eroded and potentially desorb contaminants as they move in the water column; therefore, the sediment transport processes are critical to fully understanding contaminant fate and transport in a system. Figure 2 shows a conceptual diagram of these transport processes. These processes are highly non-linear in their frequency and interaction and require a robust qualitative and quantitative description to fully understand the ultimate fate and transport of COPCs in the system.

The objective of this document is to outline a basic System Understanding for Sediment Transport (SUST) which provides a description of the sediment transport processes governing the fate and transport of contaminants in the LPR. Although a comprehensive Conceptual Site Model (CCSM) has been developed for the LPR (Appendix A, CCSM), the system understanding will be used as a tool for synthesizing and linking existing data sets and modeling analysis for answering site management questions. Additionally, the understanding will be used to develop a strategy to guide future data and modeling analysis efforts in addressing the site management questions. The conceptual understanding presented here is primarily qualitative in nature and is not intended to present a complete analysis of all data available for the system.

SYSTEM OVERVIEW

The LPR is bounded by the Dundee Dam (River Mile [RM] 17.4) and Newark Bay (RM 0). The Lower Passaic River and its watershed, including Saddle River, Second River, and Third River, define the Study Area of the Lower Passaic River Restoration Project. River depths throughout the LPR range from less than 1 m (3.3 ft) in the upper portion to almost 10 m (32.8 ft) in the lower portion of the LPR. Figure 3 shows the significant upstream decrease in cross sectional area with river mile. Flows over the Dundee Dam are the primary sources of freshwater and solids to the LPR. Table 1 illustrates the median flow and recurrence intervals of flow rates on the river. Additionally, the mouth of the river in Newark Bay is

driven by a semi-diurnal tidal water level with a range of approximately 1.5 m (4.9 ft). Salinity in Newark Bay is high relative to the freshwater inflow over the Dundee dam, especially near the bottom, but it varies in response to freshwater flow and wind (Appendix A, CCSM; Chant et al., 2009).

Table 1. Median flow and recurrence intervals for river flow on the LPR.

Return Period	Little Falls (cfs)	Little Falls (m^3/s)
Median	610	17
1-month	3900	110
6-month	4500	127
1-year	6200	175
2-year	6751	191
5-year	9968	282
10-year	12219	346
25-year	15280	432
50-year	17465	494
100-year	19808	561

ESTUARINE CIRCULATION AND RIVER FLOW

The density contrast between the freshwater inflow from the river and the saltier water in Newark Bay interacts with the tides to form a *partially mixed estuary* (Dyer, 1997). The heavier saltwater in Newark Bay tends to drive under the outgoing river water creating a salinity (and density) stratified water column throughout the lower few miles of the river (black line in Figure 4). At the same time, strong tidal currents (flooding into the river or ebbing out of it) generate turbulence that partially mixes the water column. The constantly adjusting balance between river inflow, salinity at the river mouth, and tidal mixing determines the extent of salt intrusion into the river and the structure of the two layer *estuarine circulation*. The net inflow on the bottom and net outflow at the surface typical of a partially mixed estuarine circulation are shown schematically in Figure 4.

Tidal current energy gradually decreases as the tide moves up the Passaic River, primarily due to decreasing upstream intertidal volume approaching the head of tide at Dundee Dam and frictional loss. The tidal current energy is also concentrated by the narrowing and shallowing cross-section of the river bed. As a result, flood and ebb tidal currents are significant contributors to currents in much of the river. Local combinations of tidal, riverine, and estuarine flow vary both up the river and across its width, generating strong asymmetries in near bottom flow that largely control the direction and magnitude of sediment transport.

A 3-dimensional hydrodynamic model of the LPR was developed and validated, which provides additional insight into the circulation in the LPR (HQI, 2008). Time series of combined tidal and net axial flow velocities above (tidal fresh) and below (estuarine) the limit of salt intrusion from the LPR model is shown in Figure 5. In this figure the river flow is relatively constant but the tide varies over a fortnightly cycle to illustrate the effects of the spring-neap cycle of tidal energy. In the tidal fresh river

the largest instantaneous velocities are during ebb tide because the ebb tides and river currents add constructively. In the lower layer downstream of the salt front, the estuarine circulation and flood tides add constructively, such that the highest instantaneous flows are in the upstream direction during flood tide. The estuarine circulation during neap tide is stronger than the spring tide because there is less tidal current and mixing. The lower mixing allows for stronger salinity stratification which results in a greater estuarine flow. In the surface layer, downstream of the salt front, net flows are always seaward and are stronger than in the tidal fresh river due the confinement of the downstream flow in the surface layer. Different geometries and ratios of river flow to estuarine circulation change the relative magnitudes of the flow components in different regions, but the general pattern of strongest flows during ebb tide in the river and the estuarine upper layer, and during flood tide in the estuarine lower layer, is almost always present.

To better illustrate the physical processes controlling hydrodynamics and sediment transport in the Passaic River, it is useful to examine the relative energy levels of different flow components in each portion of the LPR. As mentioned, the key forcing factors are the river flow, the estuarine circulation associated with salt intrusion, and tidal fluctuations. Additionally, wave action in the wide and shallow Newark Bay can strongly influence sediment resuspension over the shoals and subsequent transport into the LPR during flood tides. Figure 6 shows the typical situation where the river flow dominates the upper river beyond the reach of the saltwater front. This region is labeled “River Dominant”. In the tidal mid-river, the interactions between tidal currents, river flow, and estuarine circulation described above control spatial patterns in flow and sediment transport near the salt front. The region where the freshwater and saltwater interact is labeled “Mixed”. Downstream of this region, where the water column is vertically stratified, is considered “Estuary Dominant”. Wave energy is most important outside the mouth of the river, but its influence can extend slightly into the river through its effect on suspended sediment levels. Figure 7 illustrates how this scenario changes as the river flow increases. At higher river flows the salt intrusion is pushed downstream and potentially out of the river. Most of the river is dominated by strong downstream flow interacting with the tide in the lower river. The locations of the regions in these figures are for conceptual illustration and are not meant to be quantitative.

To characterize the extent of the saltwater/freshwater interaction, it is useful to define a “Salt Front”. For the purposes of the CCSM (Appendix A), this was defined as the location where the salinity at the bottom of the water column drops below 0.5 ppt (also labeled equivalently as psu in some figures presented herein). Figure 8 presents LPR model output from the simulation period of March 1995 through September 2004. The daily location of the salinity concentration of 0.5 ppt at high tide is plotted against the upstream flow rate. There is a strong relationship between river flow rate and salt front location. The median flow of 17 m^3/s (610 cfs), from Table 1, puts the high tide salt front at approximately RM 8. As the river flow rate increases, the 0.5 ppt salt front is pushed out to the lower two miles of the river. Conversely, in extremely low flow conditions the salt front can reach to RM 14 and above. One can similarly scale the upstream reach of the mixed energy zone in Figures 6 and 7 with this plot. It is noted that the 0.5 ppt functional definition of the salt front used in the CCSM (Appendix A) is based on a chemical definition. Sediment transport analyses often use a value of 2 ppt, based on physical observations of the location of the estuarine turbidity maximum (ETM) zone. The 2 ppt definition would generally have the effect of shifting the results presented here downstream slightly.

SEDIMENT TRANSPORT

The dynamic between river dominant behavior in the upper river, estuarine circulation in the lower river, and tidal currents that gradually decrease with distance upstream provides a complex interplay of processes governing sediment transport in the LPR. The important source of sediment to the system is from flow over the Dundee Dam. The Dundee Dam not only regulates the dominant flow through the system, but also provides the largest source of sediment to the system. The upper river generally behaves as a normal river with advective transport of sediments downstream.

During low flow conditions, the tidally generated currents typically resuspend some sediment during peak flood and ebb flows, which then settle back out during slack tides. The amount of surface sediment suspended and deposited during these tidal cycles is typically on a scale of a few millimeters (Sanford, 1992). The net transport of this tidally resuspended sediment is typically very slow, yet the estuarine circulation during low flow largely controls where the sediment goes. As discussed, the combination of the river flow, salinity gradient, and tidal energy in the reach downstream of the salt front results in a residual upstream flow near the bottom and downstream flow near the surface. This zone of convergence provides for increased deposition of sediment being carried upstream from the direction of Newark Bay in the lower layer during flood tides and the sediment load moving downstream from the river. This zone of elevated sediment concentrations in the water column is called the Estuarine Turbidity Maximum (ETM), and plays a key role in estuarine sediment transport. The bathymetric data in systems comparable to the LPR suggest that over the long term (i.e. decadal time scales), the ETM is a region of sediment accumulation; although, periodic high river flow and storm events (e.g. Nor'easters, tropical storms) can cause short term changes in this pattern (Geyer et al., 2000). Downstream of the ETM in deeper waters in the navigation channel are lower bed shear stress regions that will have higher probabilities of deposition which have also shown long term net accumulation. Figure 9 presents a conceptual diagram of the sediment transport processes at work in the LPR during present day low flow conditions.

During higher river flows, the zone of estuarine circulation moves downstream and the system is dominated by the strong downstream river flow. The high flows can cause sediment erosion in higher shear regions of the river (e.g. outer bends and constrictions) and deposition of the resuspended sediment in lower shear regions (e.g. inner bends) The high flow cases are characterized by a net transport of sediment out of the LPR into Newark Bay.

The following sections will illustrate the transport processes in more detail with field and modeling results.

TRANSPORT CHARACTERIZATION

These sections extend a more detailed picture of the processes in the LPR based on data and modeling. The goal of these sections is to present a better description of the river processes and provide general summary of available data.

WATER COLUMN

Much of the discussion in the previous section dealt with hydrodynamic and sediment transport processes in the water column due to river and tidal flows and estuarine circulation. A few key data sets and analyses provide excellent illustration and quantification of the water column processes. By collating these studies a more complete picture of processes in the water column can be developed.

A study implemented by B. Chant at Rutgers University in 2004 and 2005 provide an excellent baseline of water column velocity, salinity, and Total Suspended Solids (TSS) measurements in the LPR focused on better understanding sediment transport in the system. The study is summarized in a 2009 paper (Chant et al., 2009). Longitudinal profiles of salinity and TSS during low and high flow cases illustrate the dominance of estuarine and riverine processes depending on flow. The top panel of Figure 10 shows a low flow condition of approximately 1 m^3/s (35 cfs), well below the median flow rate. The salt front extends to between RM 10 and 12 with an ETM evident at the salt front. The ETM has measured TSS values of up to 50 mg/L. The range of the salt front is consistent with the conceptual model presented in Figure 6 for very low flows. The development of the turbidity maximum at the salt front illustrates that the LPR behaves consistently with our conceptual model of estuarine circulation.

Conversely, the bottom panel of Figure 10 shows measurements conducted when the river flow was 330 m^3/s (11653 cfs), greater than a 1-in-5 year flow. The salt front is pushed out into Newark Bay with high solids levels (above 50 mg/L) well into Newark Bay. These measurements illustrate a case where the river flow dominates the entire LPR and there is a strong export of sediment out of the mouth of the river.

The preliminary hydrodynamic and sediment transport modeling conducted by HQI shows similar behavior in the river. Figure 11 shows longitudinal profiles of TSS and salinity in the river during a flow rate of 51 m^3/s (1801 cfs). The salt front (bottom panel) extends to approximately RM 7 at high tide and recedes to RM 3 during low tide. The TSS shows a turbidity maximum near the salt front at RM 7. Figure 12 shows the tidally averaged velocity profile at RM 5. The profile shows a clear residual upstream velocity near the bottom and strong downstream velocity near the surface. The profiles of the salt front, TSS, and the residual velocity help to illustrate the magnitude and extent of estuarine circulation occurring in the LPR.

A contoured time series of water column data at fixed points can provide a more accurate picture of the movement of water and sediments past fixed locations in the river. Ocean Surveys, Inc. (OSI, 2009) had mooring systems measuring velocity and turbidity at RM 3 and 4 during relatively low river flow in the summer of 2009. The top panel of Figure 13 shows a time series of these two platforms. The data can be quickly organized into turbidity (a proxy for TSS) at high vs. low tide and flood vs. ebb tide. The data show that the turbidity levels are significantly higher during flood than ebb tide. The observation illustrates that there is a higher mass of sediment transported upstream during flood tide and a lower mass of sediment transported downstream during ebb tide. This observation strongly suggests upstream solids transport during low river flow.

Time series profiles of salinity and total suspended solids from moorings deployed during the Chant et al. (2009) study provide a detailed picture of the water column structure in the lower river. Figure 14 shows Acoustic Doppler Current Profiler (ADCP) and TSS measurements at approximately RM 3 corresponding to high (top) and low (bottom) river flow rates. During the high flow period, a significant drop in salinity during ebb tide (red and blue lines) is accompanied by a large increase in TSS (solid contours). The data show high TSS during ebbing tides denoting a strong downstream transport of TSS during this elevated flow event. The low flow period (bottom) shows reduced TSS levels and a strong diurnal salinity signal. During this normal period of estuarine circulation the TSS levels are higher on flood tide than ebb tide denoting a net upstream transport of solids.

Chant et al. (2009) calculated the daily average fluxes at the mooring near RM 3 (Figure 14) over approximately 7 months of measurement in 2004 and 2005 using the velocity and TSS measurements. Figure 15 shows a summary of the flux data as a function of tidal range and river discharge (flow rate). The hotter (e.g. orange) colors denote net upstream transport while the cooler colors (e.g. blue) denote net downstream transport. The summary of data shows that as river flow drops, estuarine circulation is responsible for the upstream transport of solids at the mooring location. As the river flow increases, the net flux of sediments is downstream as river flow disrupts the estuarine circulation. These data can be collapsed into the approximate curve as a function of flow rate only shown in Figure 16, which was adapted from the Chant et al. (2009) data. The curve illustrates that at river flow rates below approximately 30 m^3/s (1059 cfs), the net sediment transport at RM 3 is upstream. Above 30 m^3/s (1059 cfs), river flow begins to dominate the signal and the net sediment transport is downstream. At high river flows (greater than ~ 200 m^3/s or 7063 cfs) the net downstream transport is over 100 times higher than the upstream transport during low flow, yet these events occur during a much shorter time frame. It is important to note that this analysis is limited in that it is based on measurements at one location during limited time periods.

MASS BALANCE

Using the transport information, a conceptual mass balance in the river can be constructed. Generally, the mass balance in the river can be defined as:

$$\text{Upstream Load} + \text{In River Erosion} - \text{In River Deposition} = \text{Net Transport Out}$$

The net transport out term can be positive or negative for upstream transport. Based on sources of sediment to the river a qualitative diagram of the two conditions can be illustrated as in Figure 17. During low flow conditions we have a low level of net sediment transport upstream and a very low input from the river. During these conditions a net deposition balances out the net influx of sediments. During a high flow situation, the upstream loadings coming over Dundee Dam increase significantly and the net transport out of the LPR also increases significantly. Some unknown amount of greater erosion and deposition occurs in the river.

By using the upstream river loading estimates developed by HQI for the Dundee Dam and other tributaries with the sediment transport approximation for the mooring near RM 3 from Chant et al. (2009), we can look at total cumulative sediment transport and net deposition of sediments in the river. It is important to note that these functions are approximations based on discrete datasets during varying time periods and have uncertainty associated with them; therefore, these calculations are meant to be more qualitative than quantitative. Figure 18 shows flow rate and estimated cumulative transport out of the river near RM 3 from October 1994 through September 2005. The bottom panel shows cumulative river input from the Dundee Dam and tributaries and the estimated transport near RM 3. The figures show that during low flow periods the net input from upstream is negligible while the transport from the Bay into the river causes a net upstream transport. According to these estimates, the upstream transport occurs approximately 63% of the time. The divergence of the two lines in the bottom panel shows material trapped in the river during these time periods. The net sediment deposition during this time period is 1.7×10^5 MT, or 47% of the load coming in from upstream. It is important to note that these values are based on a few discrete time periods of measurement and are for general illustration purposes only.

In order to help validate the conceptual understanding and the preliminary sediment transport model developed by HQI, the water column fluxes calculated in the model can be examined. Figure 19 shows the daily water column solids transport vs. flow rate at 8 stations in the LPR. The spatial summary shows that during low flow rates there is a significant upstream sediment transport (points on the lower half of each graph) in the river miles most experiencing the extent of the salt front (RM 4.7 – 8.1). Above RM 14.6 there is little or no upstream transport of solids. As the flow increases above 100 m^3/s (3531 cfs), the river shifts to strong downstream transport. The plots illustrate that the strongest estuarine (i.e. upstream) delivery of sediment to the LPR occurs at the locations of the salt front and ETM.

MORPHOLOGY

To better understand the long- and short-term behavior of the sediments in the LPR, it is critical to examine the morphologic behavior of the river. The river has been significantly modified through dredging over the past century. Figure 20 shows the depth of the river channel based on a 2004 bathymetric survey as well as the original project depths (Appendix A, CCSM). It is important to note the original project depths were 3 m (10 ft) upstream of RM 8. Sediment accumulation of 4.8 m (15 ft) or more has occurred below RM 8 while changes have apparently been much less above RM 8. Since RM 8 is also the median extent of estuarine circulation, it is reasonable to conclude that the upstream transport of sediments has been effective at filling in the estuary.

An illustration of the infilling of the LPR after cessation of dredging is shown in Figure 21. This figure shows approximate bathymetries of the LPR over time, derived from historical charts by Chant et al. (2009). Infilling after dredging ceased did not occur uniformly, but was focused at the upstream end of the dredged channel and worked its way downstream over time. This is consistent with geological understanding of the long term fate of drowned river valley estuaries in which sediments infill most rapidly near the limit of salt intrusion (the vicinity of the turbidity maximum). Chant et al. (2009) and MacCready (1999) have surmised that the deepening of channels due to dredging or other processes is accompanied by a more landward extent of salt and the estuarine circulation, which results in dispersion of sediments further upstream. Thus, it is likely that the rate of deposition has varied spatially as well as temporally as the LPR has readjusted towards its equilibrium morphology.

Additional bathymetric analysis of surveys from 1989 to 2004 in the LPR provides validation of the infilling trend over the recent term. Over the time period, the average infill rate is estimated to be 51,000 m^3/yr (66,700 yd^3/yr) (Appendix A, CCSM). The surveys analyzed also showed that approximately 90% of the material has deposited within the lower 7 miles of the river. These long term observations are consistent with the overall sediment transport conceptual model. In the shorter term, year to year bathymetric surveys showed high variability in erosion and deposition patterns. The patterns are heterogeneous spatially and temporally and do not correlate well with timing of the more erosive high river flow. More analysis of the short-term survey comparisons is needed to understand the uncertainty associated with the measurements before they can be used with confidence to quantify short-term erosion or deposition trends in the river.

To better understand the finer scale features of sediment transport in the river, it is useful to define morphologic regions of the river. Using the 2008 high resolution multibeam survey data, eight different morphologic features were used to describe the commonly observed features in the LPR. The regions are:

1. Abutment – Hard structures such as bridge piers or scour protection in the vicinity of bridges that can alter flow and scour patterns.
2. Abutment Scour – Readily identifiable scour due to abutment features.
3. Broad Shoal – This term generically applies to broad mudflats and/or point bars typically located on the inside of river bends.
4. Island – In the upstream portions of the river, above water island features are present.
5. Margins – These are broad channel margins near the shoreline that are often similar to the broad shoals but could also be anthropogenic shoreline features.
6. Smooth Channel – The channel region is the broad relatively flat central channel present through much of the river. Although there are perturbations, the overall feature is considered smooth here.
7. Deep Scoured Channel – These channel regions typically occur on the outside of river bends where there is enhancement of velocities, and shear stress, resulting in the maintenance of a deeper scoured feature at these locations. The delineation is not meant to suggest that these are long term net scour features.

These qualitative morphologic definitions are intended to help understand the general lateral and longitudinal features in the river. Identification of these features can help to better understand transport trends and more effectively design remediation. Figure 22 through Figure 24 illustrate the multibeam survey data and the identified morphologic regions of the river in the vicinity of RM 2, RM 4, and RM 6. The most important feature that stands out in the delineation of the morphologic regions is that the point bar deposition/ mudflat regions on the inside bends where the velocities are lower and the deeper channel features on the outside bends fall in line with what one expects in a flow channel. This behavior can be observed nearly uniformly throughout the river. The presence of these features suggest that during high river flow events, the highest shear stresses and higher probability for erosion can be expected in the deeper channels and the lowest shear stresses and higher probability for deposition can be expected on the shoals. Additionally, the long-term presence of the features shows that the tidal currents maintain the channel morphology during periods of net sediment influx from the direction of Newark Bay.

Both typical and atypical bedforms exist in the channels of the LPR. Figure 25 illustrates bed features near RM 3 and RM 8. Near RM 3, where the sediment bed is predominantly fine material, typical sand waves and ripples do not form; although, there are lumps of material at the river bed (possibly large detritus mounds or clumps of stiff material of unknown origin) that show a smooth deposition on the upstream lee of the feature. The feature suggests a net upstream direction to near-bed sediment transport at the time of the survey. The RM 8 bedforms are typical of uniform sand waves moving downstream. The shape of the feature has a dominant downstream directionality. The bedforms suggest that the bidirectional flow in this region was not significantly affecting the bed in this region at the time of the survey (low flow).

SEDIMENT BED

Looking at and into the sediment bed can provide information on the long- and short-term behavior of sediments in various regions of the river. One of the most basic sediment bed properties is the particle size. In addition to a large number of surface grabs collected as part of the 2005 field effort, a side scan

survey was conducted. The particle size samples were used to calibrate a bottom textural classification based on the side scan reflectivity. The data provide a broad delineation of surface rock, gravel, sand, and silt in the river. These are broad definitions and often don't distinguish between more detailed classifications such as sandy silt or silty sand. Figure 26 shows an overlay of the bottom type on the river. The lower eight miles of the river are dominated by silt material with pockets of silt and sand. River mile 8 shows a dramatic shift to sand and gravel sediment with pockets of silt. Figure 27 shows a close up of this fairly sharp transition. Although the side scan data provide a continuous delineation, it is based on surface conditions which can vary rapidly with flow so some level of variation can be expected. The transition at RM 8 is again associated with the extent of the salt front and estuarine circulation propagation which delivers and traps fine sediments at the bed. The reasons for the coarser sediment size upstream of RM 8 are likely a combination of winnowing due to high river flows and the proximity of bedrock and potential sand and gravel sources to the bed of the river in the upstream regions.

The 2008 CPG low resolution core data can be used to calculate percent fines at each core location (material less than 63 micron size). These values are plotted over the side scan interpretation in Figure 28. The silt identification is consistent with cores containing over 50% fines. Generally material with over 50% fines is considered to be cohesive even though they may contain significant amounts of sand. It is important to note that although the side scan interpretation identified many of these areas as silt, they may be sandy silt or silty sand in a more detailed classification. Both the original surface grabs from 2005 and the 2008 cores show that there are significant silty sand regions in the lower river, yet these sediments are still generally classified as fine and cohesive.

Cesium-137 (Cs-137) profiles in cores collected as part of the 2005 CCSM sampling provide a good picture of historic deposition trends in the lower river. The 2005 cores were collected at five locations in the river which are shown in Figure 29 and Figure 30. The peak of Cs-137 activity is referenced as the peak of atmospheric nuclear testing in 1963. The broadest shoal/point bar at RM 2.2 has the deepest peak of Cs-137 suggesting the highest deposition rate. All of the peaks are below 1 m (3.3 ft) with the exception of the core at RM 7.8 which is adjacent to a scour depression near a bridge abutment. The trend in these cores provide another line of evidence suggesting that the long term river behavior is consistent with our conceptual model of infilling throughout, but modified by morphologic features.

An additional data source which provides information on the river sediments is the 2005 SPI camera survey. The purpose of the SPI survey was to characterize the physical and biological condition of surface sediments and assess the river's intertidal and subtidal benthic habitats by using a camera prism that slices into the sediments providing an in-situ view of the sediment. Prior to June 2005 there was a large flow event that appears responsible for delivering a large magnitude of sediment to the river. The SPI camera can be used to identify the most recently deposited sediment horizon at different locations. Figure 32 shows images and points of the SPI camera transect at RM 3.9. The inside bend of the river had the highest recent deposition of 12.6 cm (4.96 in) and the image showed the deposited material to be composed of macro-organic leaf and stick detritus. The deep channel of the river had a low recent deposition of 1.9 cm (0.74 in) and shows a much more uniform sediment column of sediment with anoxic sediment below a surficial oxidized layer. These data not only support the observation of cross-channel gradients in transport and morphology, but also show that detritus plays a potentially significant role on transport in the river. It is important to note that the SPI camera, particle size, and textural data provide only a temporal snapshot that is dependent on the river flow conditions in the months preceding the

collection of each data set; therefore, there is expected to be some variation in the specific trends noted here.

SUMMARY

A conceptual model of the interplay of estuarine circulation and river flow has been developed here. The importance of both of these processes on sediment transport during high and low flow conditions has been discussed and illustrated. Field and modeling data can be used to support the conceptual model of transport in the system and provide some quantification of these processes and their relative importance. Additionally, morphologic and sediment bed data can be used to construct a more detailed spatial picture of what is occurring in the river. The key qualitative concepts during low-flow conditions, dominated by estuarine circulation and upstream sediment transport, and high-flow conditions, where downstream river flow dominates, are summarized in Figure 33 and Figure 34, respectively.

Generally the conceptual transport model can be characterized by the following points:

- The LPR typically has tidal delivery of sediment from the direction of Newark Bay into the LPR during low flow conditions due to estuarine circulation
    - The delivery of sediment is generally limited to the lower 8 miles
    - Tidal mixing due to erosion and deposition of the surface sediment (on the order of mm [Sanford, 1992])
    - The highest shear stresses in the deep channels maintain the channels while lower shear stresses on the shoals/mudflats maintain those features
    - Based on analysis of the Chant et al. (2009) data the upstream transport of sediment occurs at flows greater than the median flow, suggesting that upstream transport occurs the majority of the time. Although the transport direction may be upstream most of the time, the analysis shows that the cumulative upstream transport of sediment is less than the cumulative downstream transport during high flow events.
- During elevated flows, the river flow in the LPR dominates and there is a net flux of sediments out of the river to Newark Bay
    - During elevated river flow conditions some portion of the unconsolidated sediment delivered form the Bay during tidal action is resuspended and transported into the lower miles of the LPR and the bay
    - Thick mats of organic detritus play a definite, yet un-quantified, role in sediment bed elevation changes in the LPR
    - The net flux of sediment during high flow events is orders of magnitude larger than upstream tidal delivery of sediment from the Bay
    - The cumulative effect of high and low flow events on transport from 1994 to 2005, based on preliminary estimates of transport, was an accumulation of 47% of the material coming into the river from upstream sources.

- Long term transport has resulted in net deposition in the river coupled with a net efflux of sediment from the river
    - Dredging in the 1940's disrupted the preferred equilibrium of the system and has resulted in strong infilling of sediment
    - Based on infilling rates over time from USACE and other surveys, the deposition rates in the lower miles of the river have decreased over time as the system approaches a quasi-equilibrium. The observations are physically consistent with the conceptual model of reduced channel size decreasing overall deposition potential.
    - The large events provide energy for erosion of the sediments. The potential for erosion is dependent on location in the river, strength of the event, and properties of the sediments.
    - More recent sediment deposits will generally be more mobile.
    - In general the long term quasi-equilibrium, once achieved, is expected to keep up with sea level rise.

Some key questions for consideration in contaminant transport and remedial evaluation can be developed from this study along with lines of suggested evidence to address the questions.

1. On the long term track, where is the LPR relative to its quasi-equilibrium?
    - Morphologic and bathymetric change analysis
    - Analysis of chemistry profiles both horizontally and vertically
    - Long term modeling to predict the trajectory of the river
2. In the present state and into the future what levels of sediment bed change and water column flux variation due to erosion and deposition can be expected in the LPR sediments during typical conditions and large events?
    - Analysis of physical sediment data (e.g. chemistry, SPI, Sedflume)
    - Continued water column measurements of sediment flux
    - Morphologic and bathymetric change analysis
    - Short term modeling to predict the magnitudes of events and spatial distributions of erosional and depositional behavior.

DATA ANALYSIS GAPS

Particular data sets were not included in this analysis due to the availability, state of data reduction, or relevance to this document. To the authors' knowledge, none of the datasets conflict with any conclusion presented herein. These data sets include:

- CPG 2009 fall physical water column monitoring data

- TSI summer 2009 water column data
- Other academic and gray literature sources of data regarding the Passaic River and Newark Bay Complex.

A sediment transport model calibration strategy is presently being drafted that will address use of these data sets, among others, in future modeling efforts. This document will be iteratively updated with new information as these data sets are analyzed.

REFERENCES

Chant, R., Fugate, D., and Garvey, E. (2009). “The shaping of an estuarine superfund site: roles of evolving dynamics and geomorphology”. Submitted for publication in Estuaries.

Dyer, K. R. 1997. Estuaries: A Physical Introduction. 2nd ed. John Wiley & Sons, Chichester, England.

Geyer, W. R., J. H. Trowbridge and M. M. Bowen (2000). "The dynamics of a partially mixed estuary." Journal of Physical Oceanography 30: 2035-2048.

HydroQual, Inc. (HQI) (2008). “Lower Passaic River Restoration Project and Newark Bay Study – Final hydrodynamic modeling report.” US Environmental Protection Agency – Region 2. Us Army Corps of Engineers Contract No. DACW-02-D-0003 (available on www.ourpassaic.org).

MacCready, P. (1999). "Estuarine Adjustment to Changes in River Flow and Tidal Mixing." Journal of Physical Oceanography 12:708-726.

Ocean Surveys, Inc. (OSI) (2009). “Oceanographic in-situ and real-time data acquisition program, Passaic River, Newark, NJ”. OSI Report No. 09ES045. Prepared for Tierra Solutions, Inc.

Sanford, L. P. (1992). "New Sedimentation, resuspension, and burial." Limnology and Oceanography 37(6): 1164-1178.

FIGURES

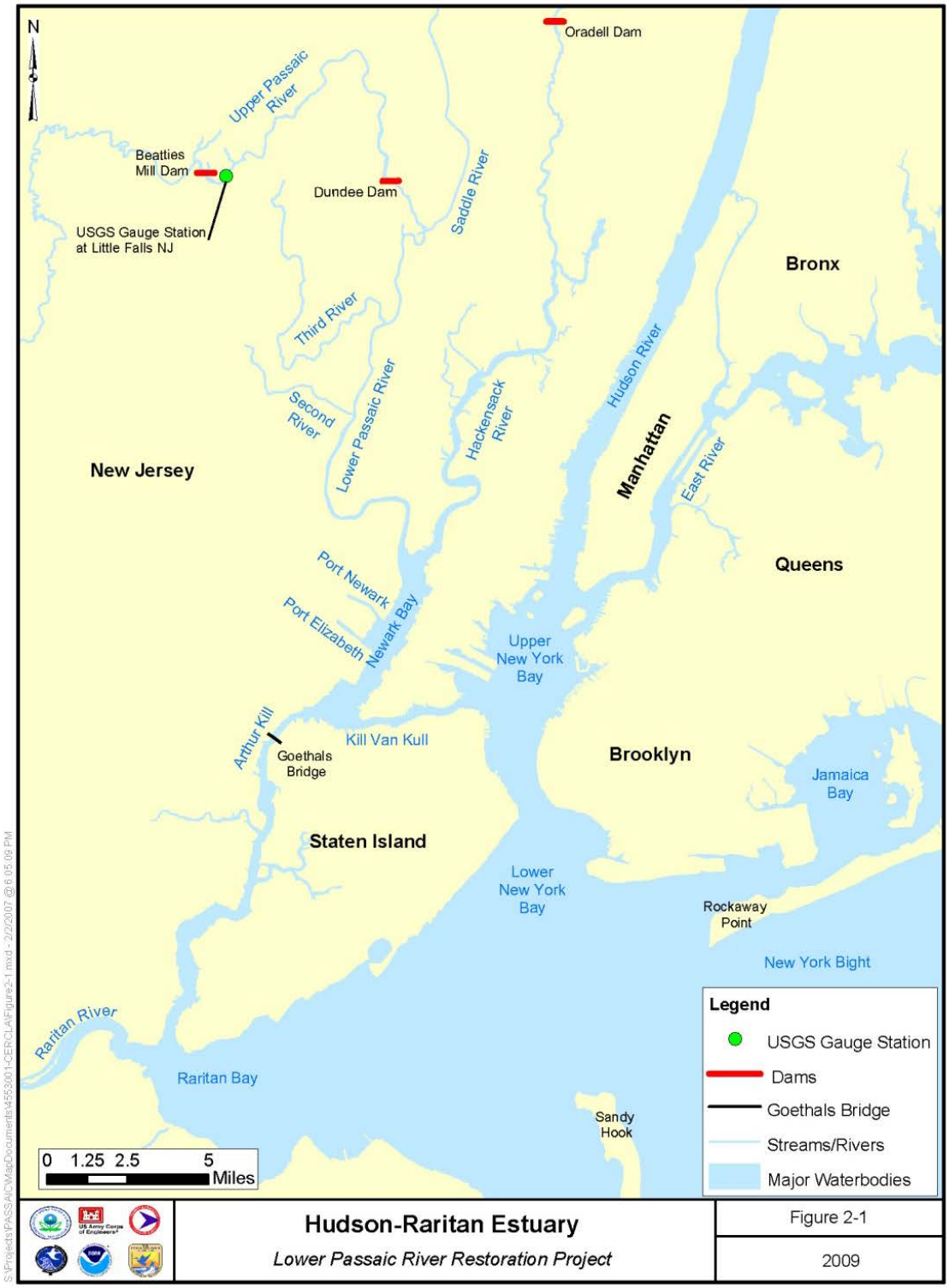

Figure 1. Map of the Lower Passaic River region (Appendix A, CCSM).

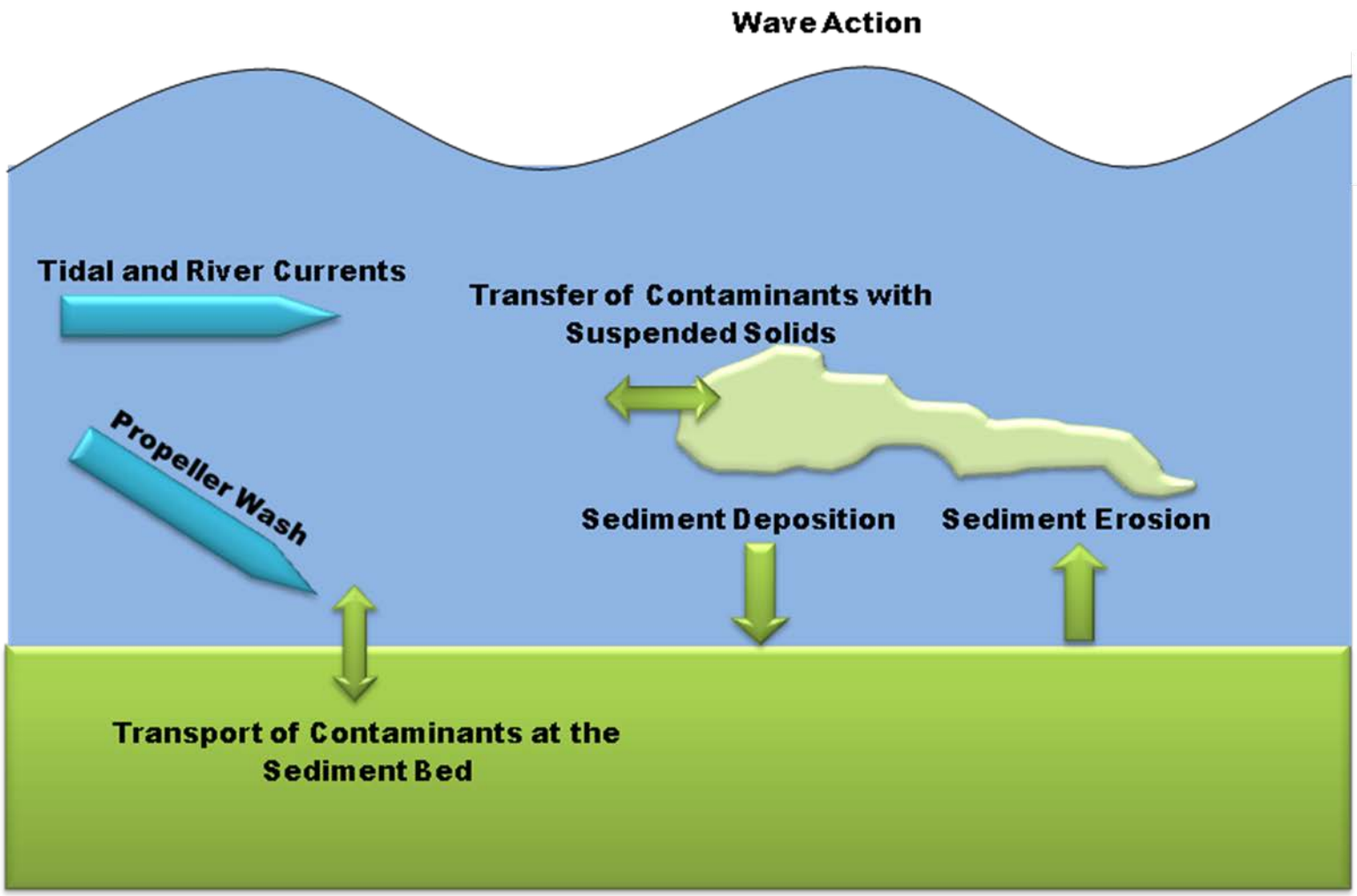

Figure 2. Conceptual diagram of processes related to sediment and contaminant transport.

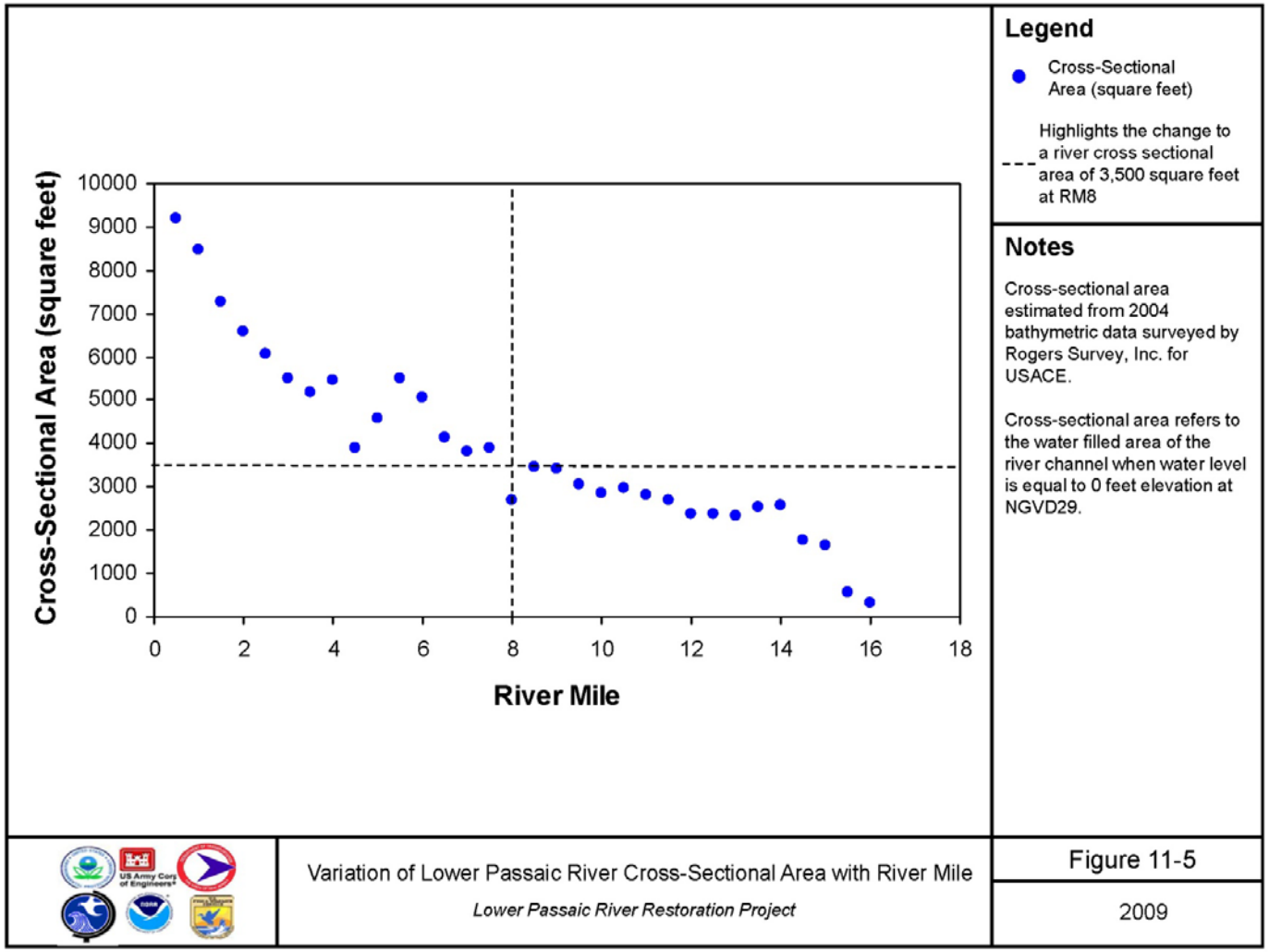

Figure 3. Variation in river cross-sectional area with river mile numbered from river mile 0 at the mouth (Appendix A, CCSM).

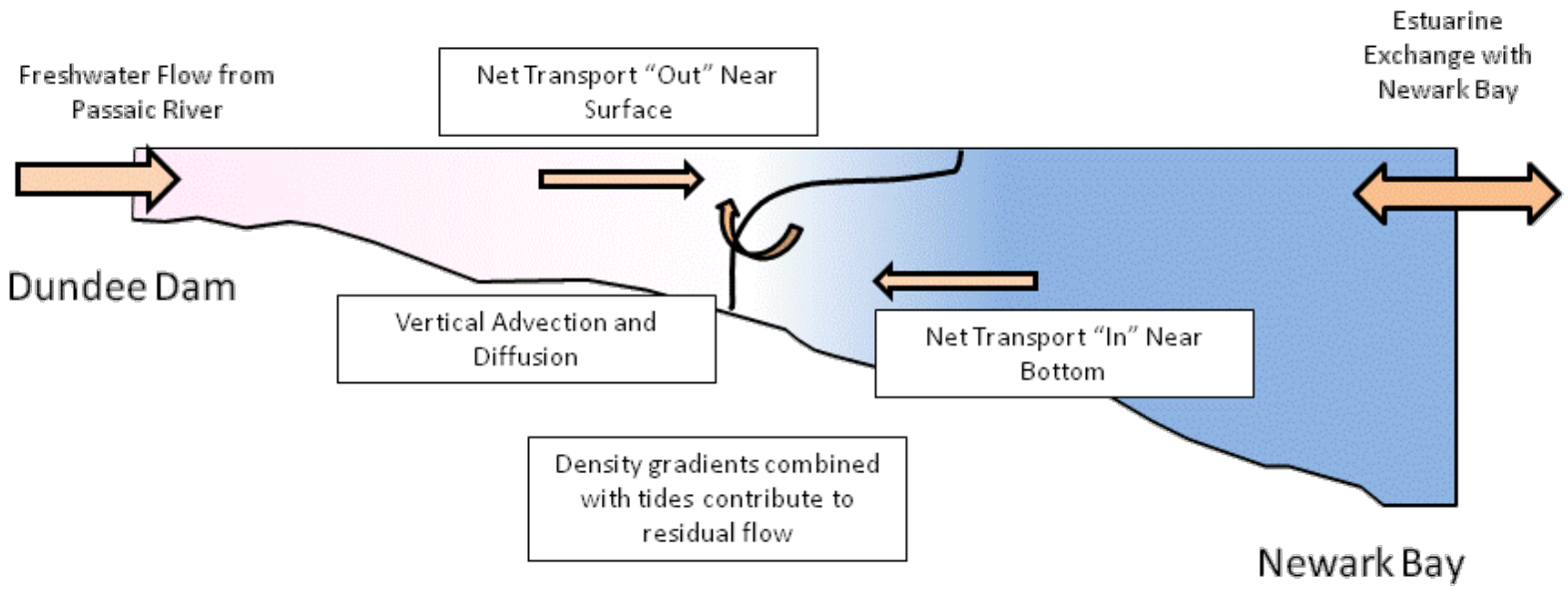

Figure 4. Estuarine processes active in the Lower Passaic River, a partially mixed estuary.

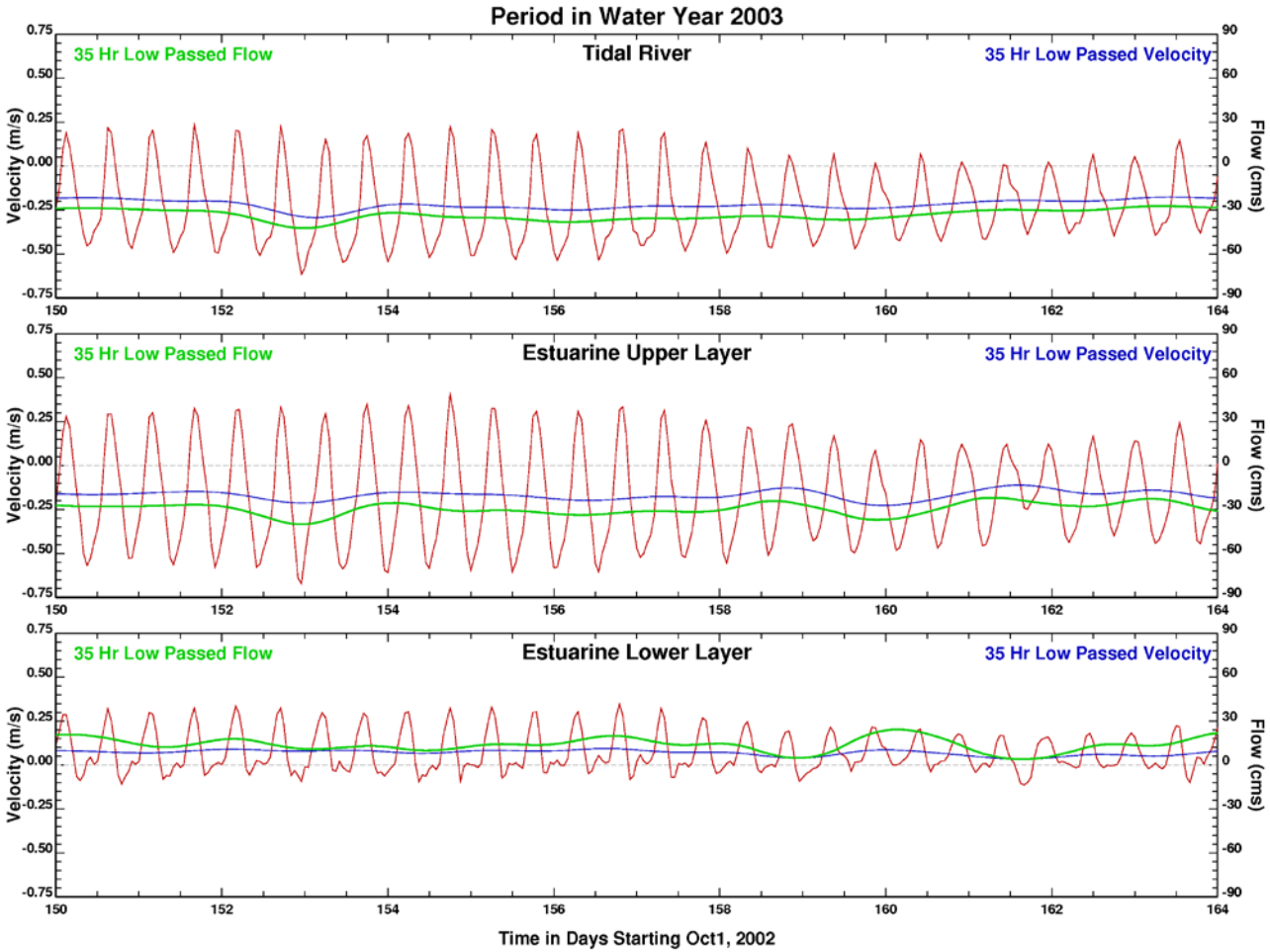

Figure 5. Time series of tidal (red), tidally filtered velocities (blue), and tidally filtered flow (green) from the LPR hydrodynamic model (HQI, 2008), in the tidal fresh region (upper panel) and the estuarine region (lower two panels). In these plots positive velocities are in the flood direction (up-river) and negative velocities are in the ebb direction (down-river).

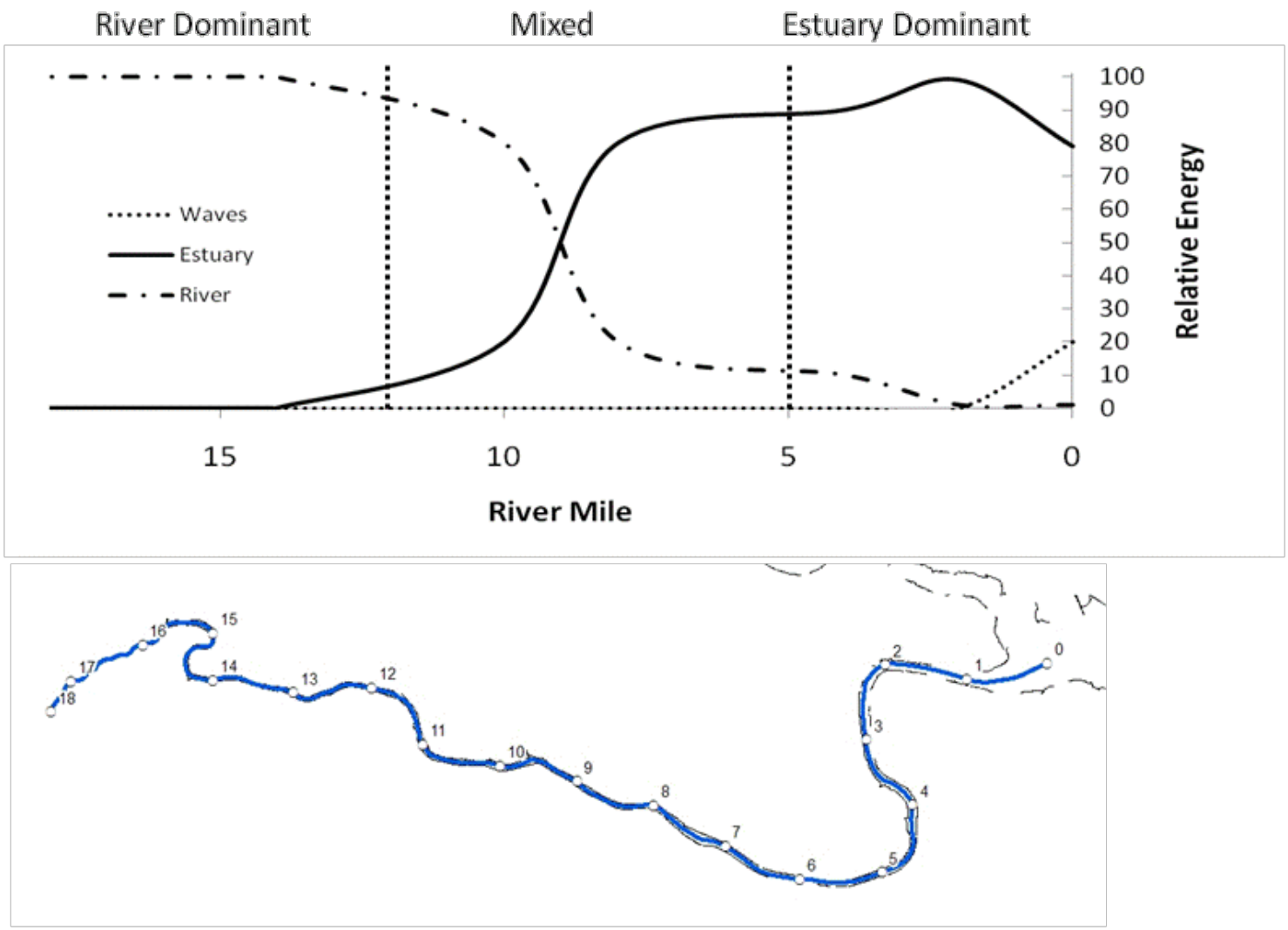

Figure 6. Conceptual contribution of three forcing factors relevant to transport in the Lower Passaic River. The figure represents median flow conditions at the Dundee Dam.

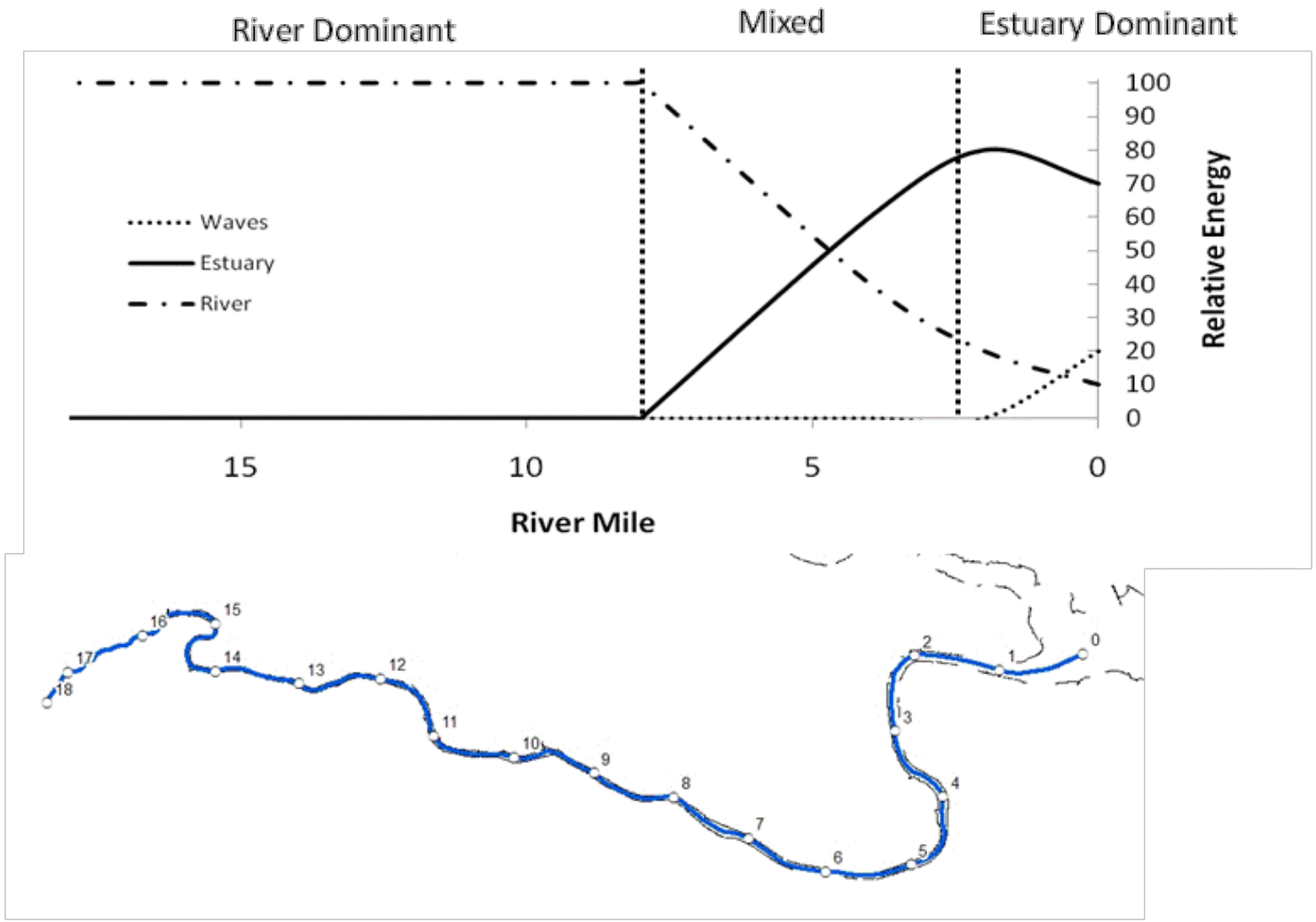

Figure 7. Conceptual contribution of three forcing factors relevant to transport in the Lower Passaic River. The figure represents elevated flow conditions at the Dundee Dam.

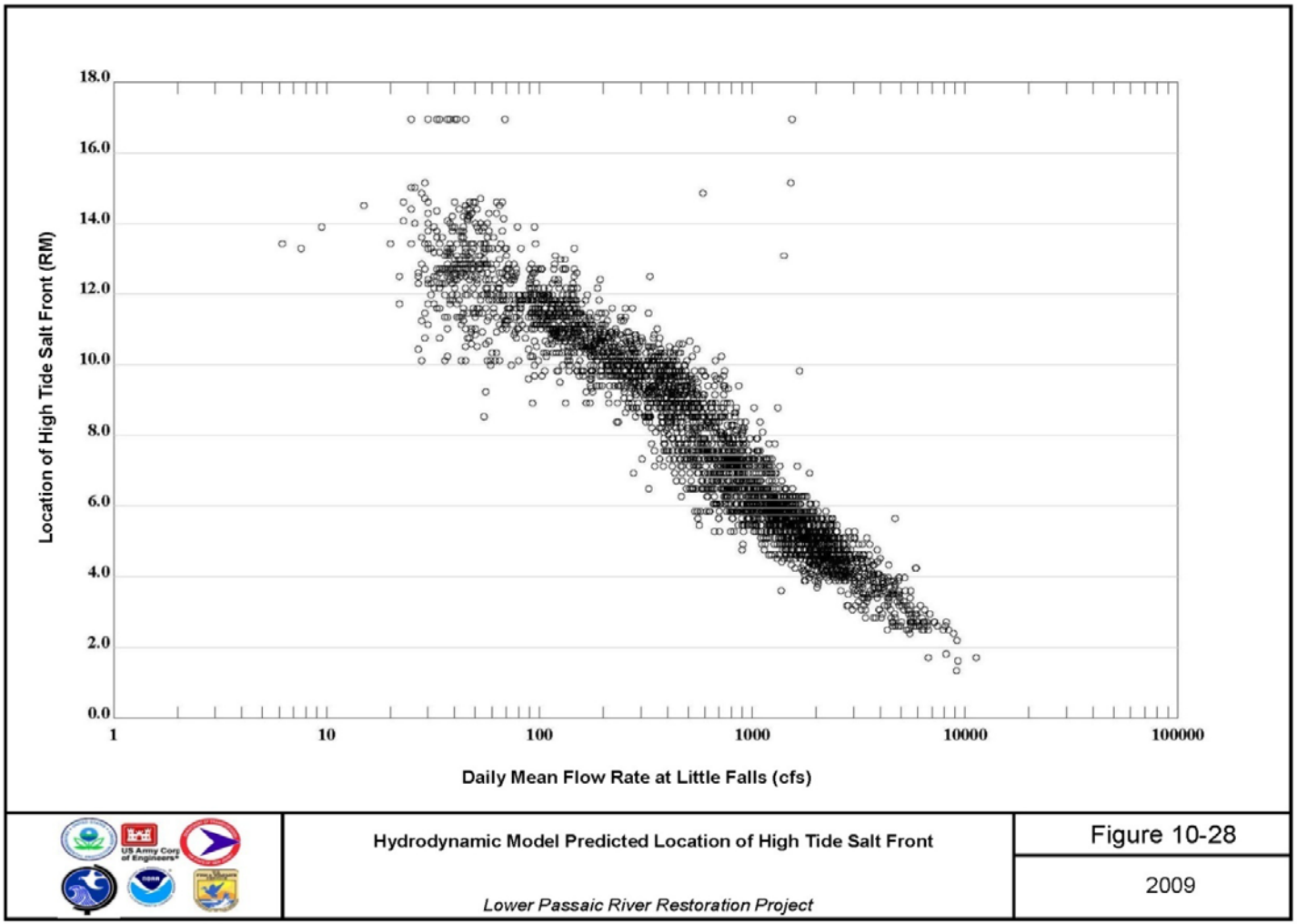

Figure 8. Location of high tide salt front as a function of flow rate determined from the HQI hydrodynamic model (Appendix A, CCSM).

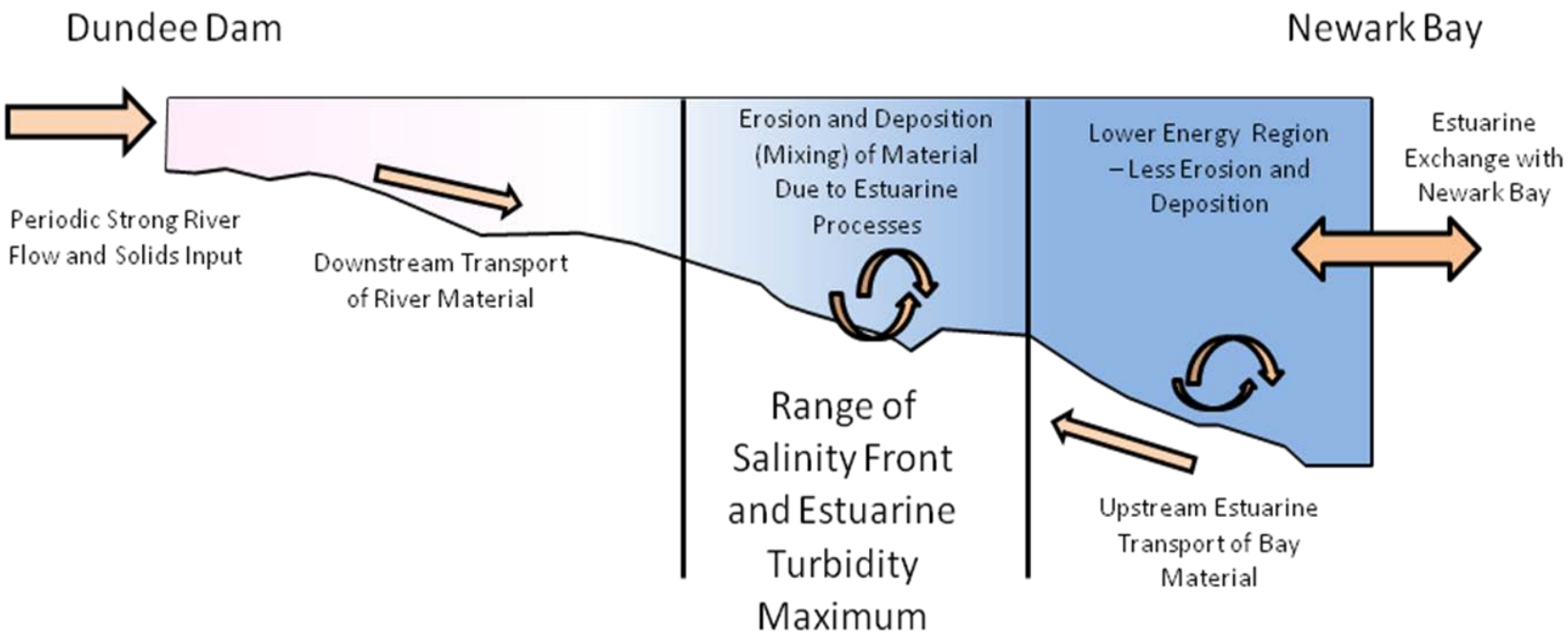

Figure 9. Estuarine and sediment transport processes active in the Lower Passaic River.

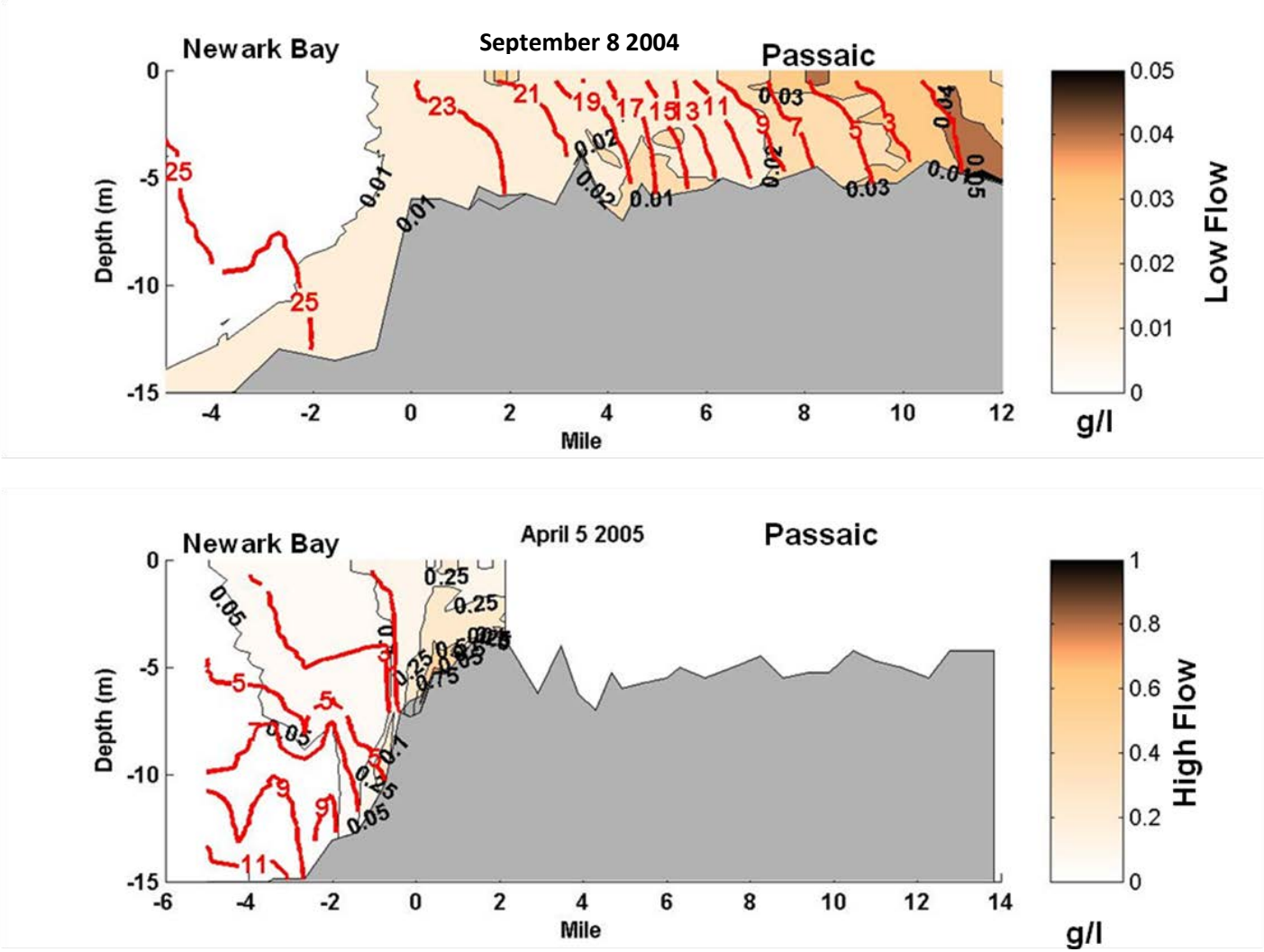

Figure 10. Longitudinal profiles of salinity and total suspended solids from Chant (2009) corresponding to 1 and 330 m^3/s river flow rates respectively.

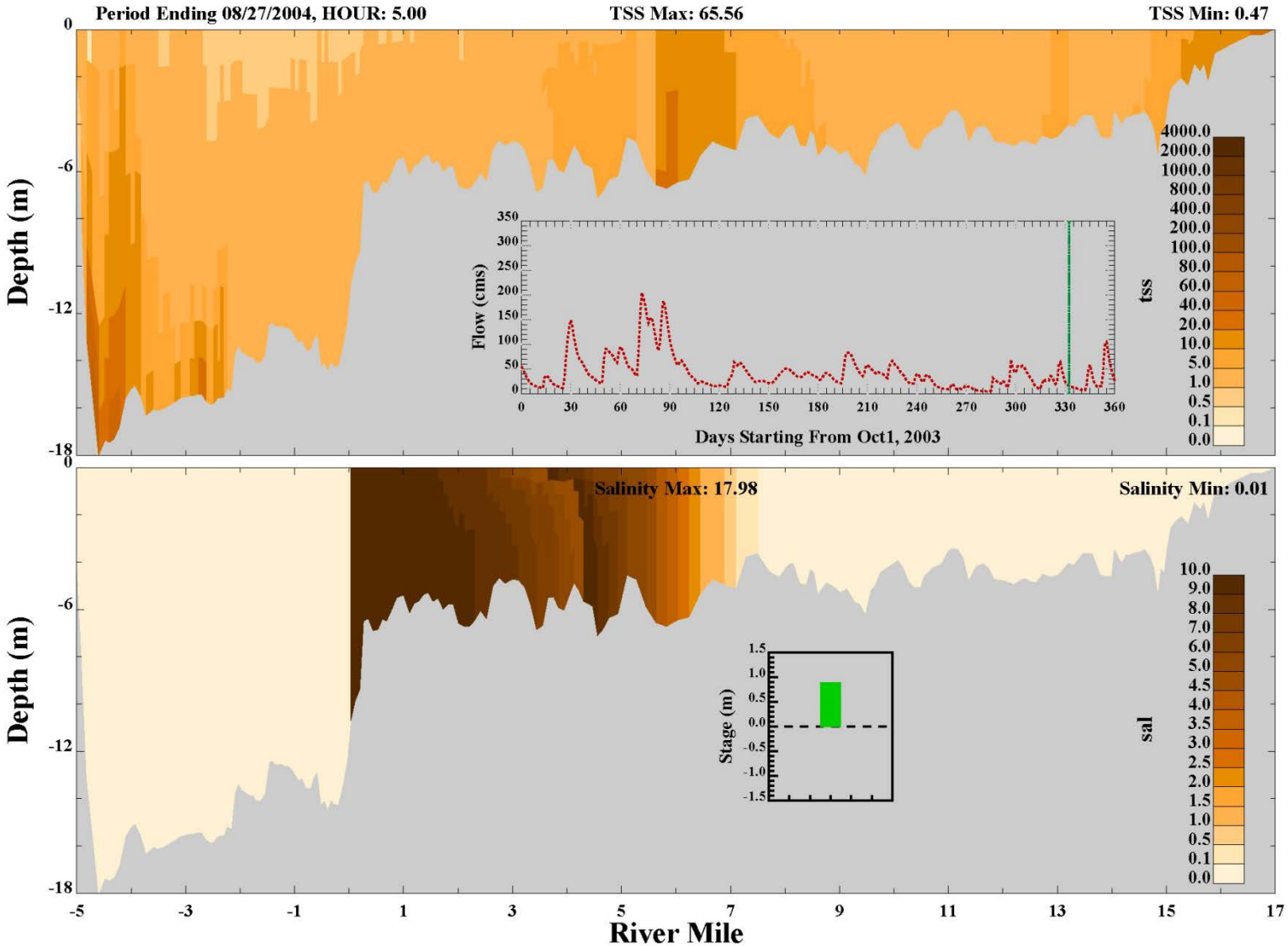

Figure 11. Longitudinal profiles of TSS (top) and salinity (bottom) during low flow conditions in August 2004 from preliminary HQI hydrodynamic and sediment transport model.

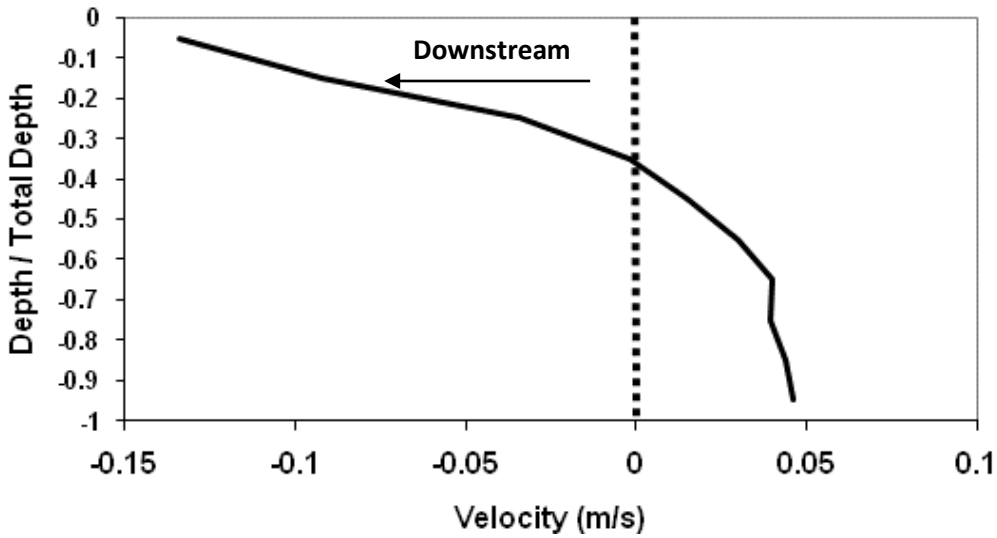

Figure 12. Tidally averaged velocity profile during low flow conditions in August 2004 from preliminary HQI hydrodynamic and sediment transport model. The profile is located at river mile 5. Negative velocity is directed downstream.

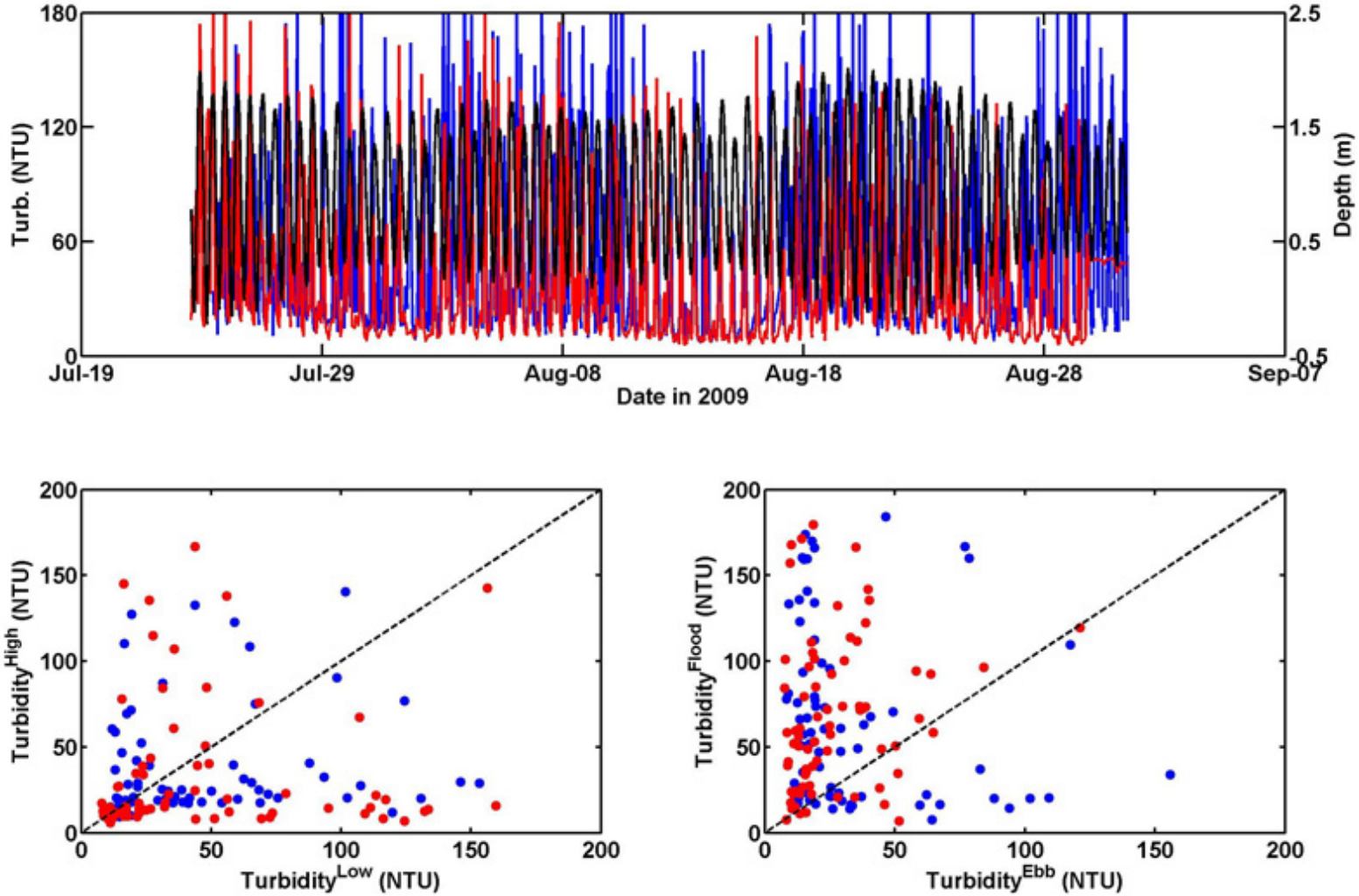

Figure 13. Time series of OSI turbidity data from two moorings (top). Plots of high vs. low tide turbidity and flood vs. ebb turbidity (bottom).

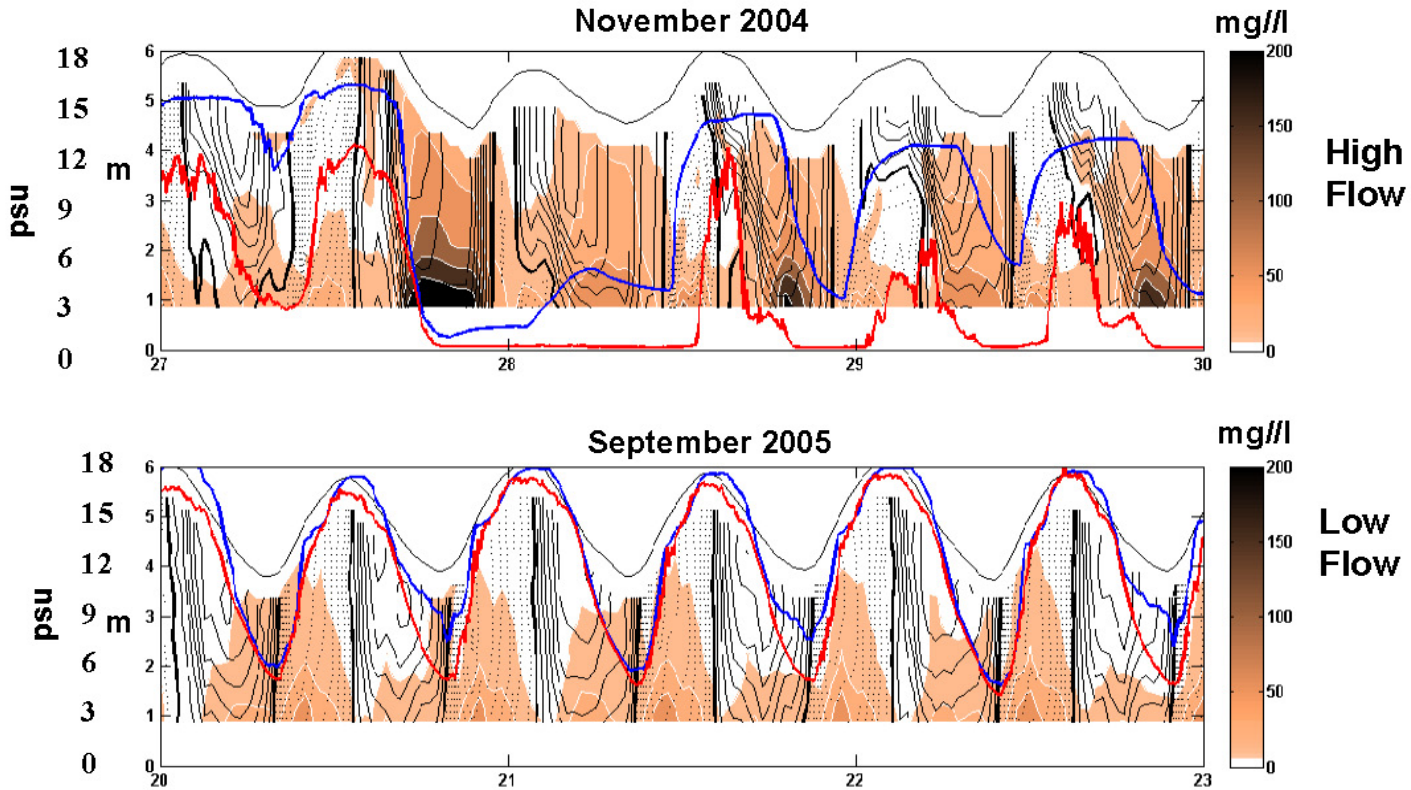

Figure 14. Time series profiles of salinity (red lines are surface and blue lines are bottom of the water column) and TSS (solid contours) near RM 3 from Chant et al. (2009) corresponding to high and low river flow rates respectively.

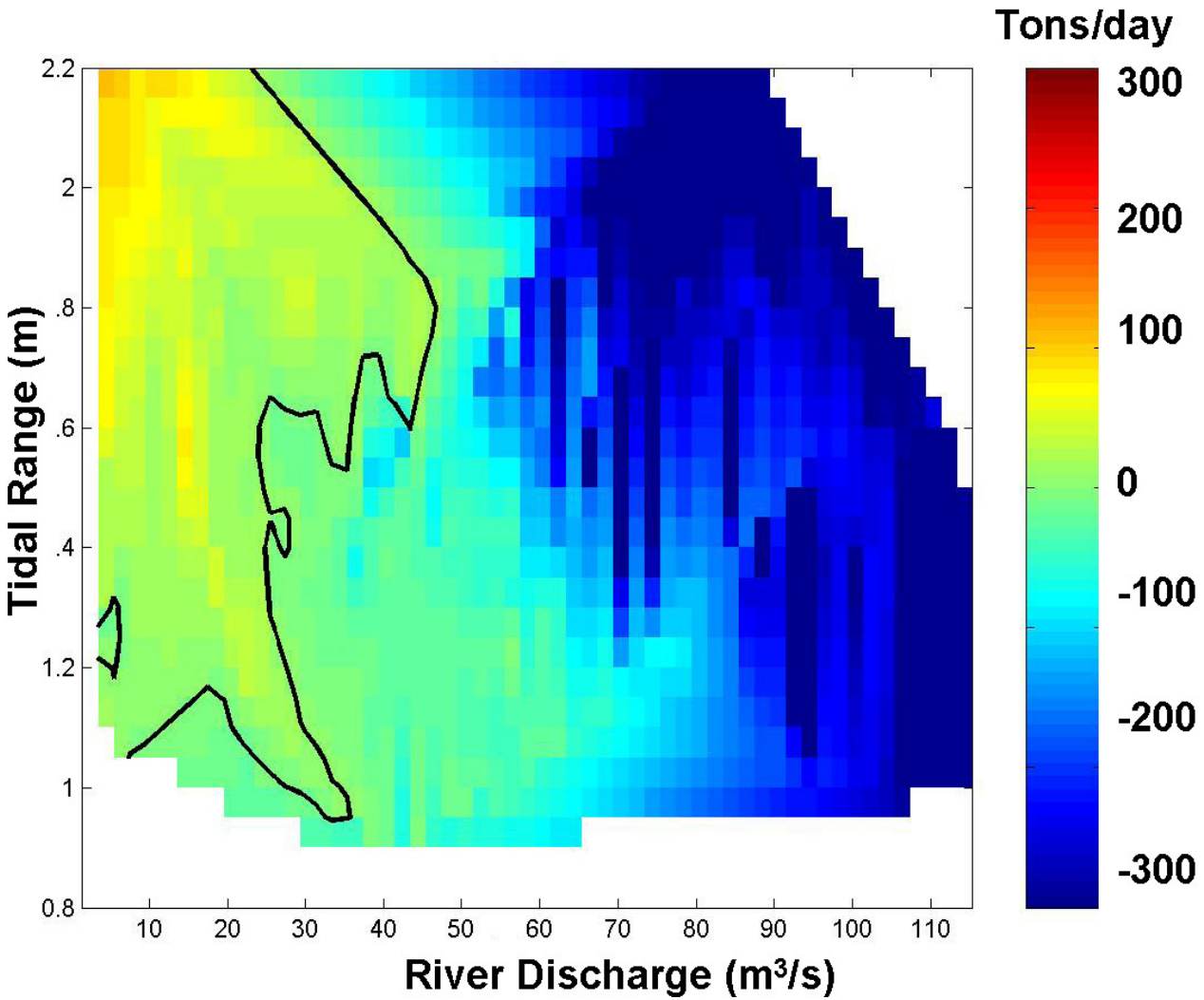

Figure 15. Sediment transport (positive is upstream) as a function of tidal range and river discharge (flow rate) estimated from current meter and backscatter measurements near RM 3 (Chant et al., 2009).

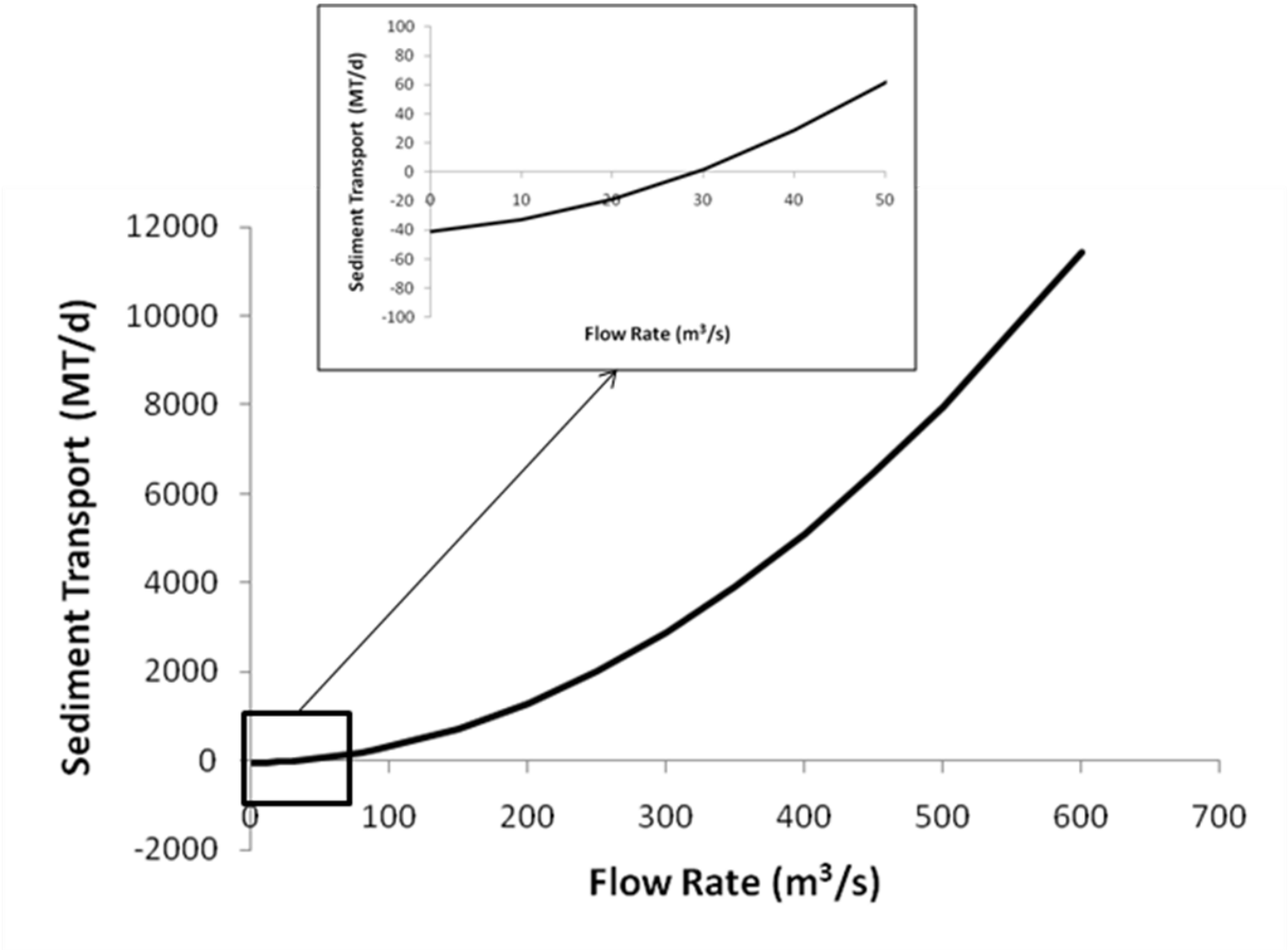

Figure 16. Sediment transport (negative is upstream) estimated as a function of river flow rate near RM 3 (Chant, 2009).

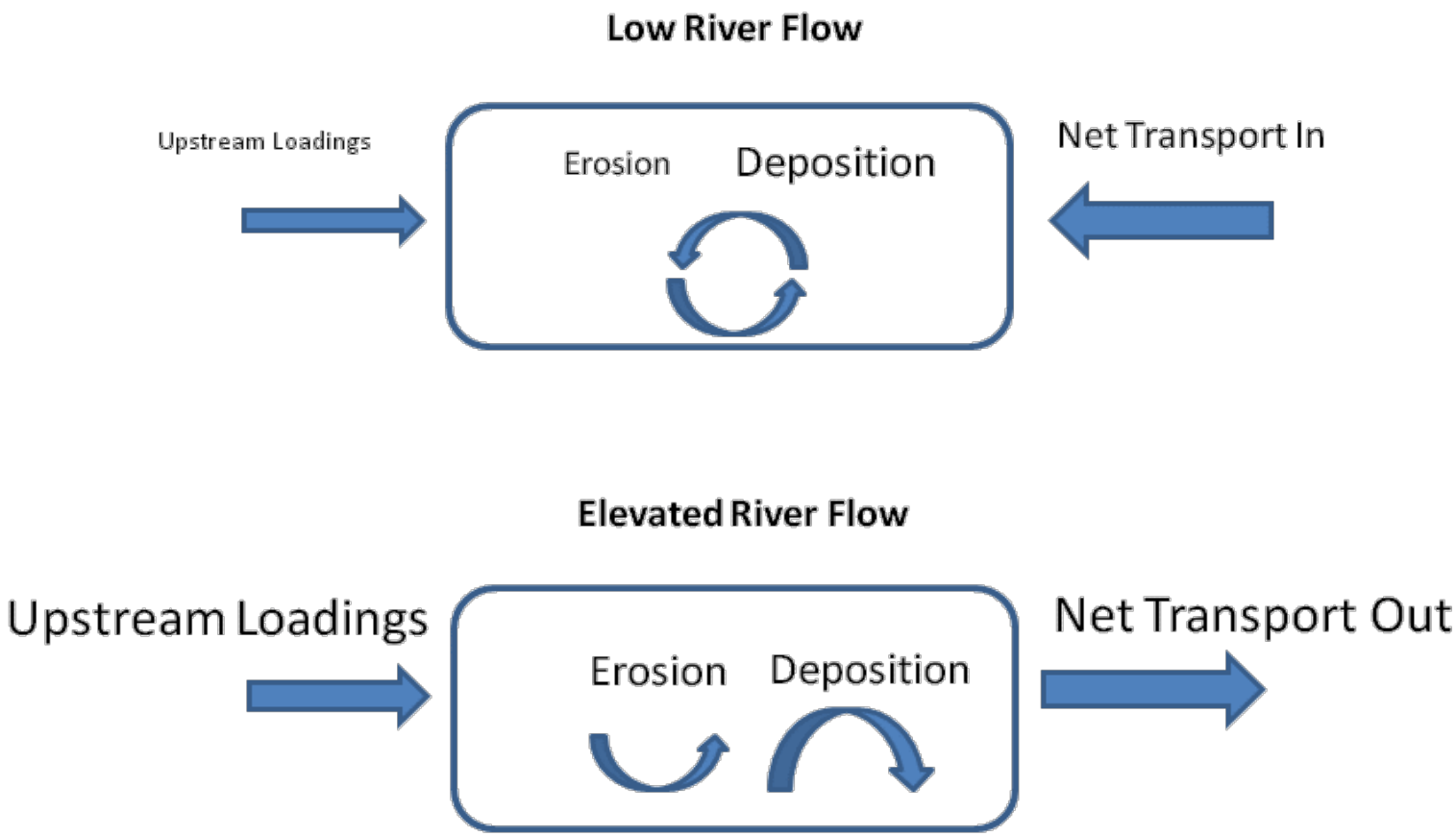

Figure 17. Sediment balance during low and elevated river flow periods. The size of each component is relative to the contribution of each term in the balance.

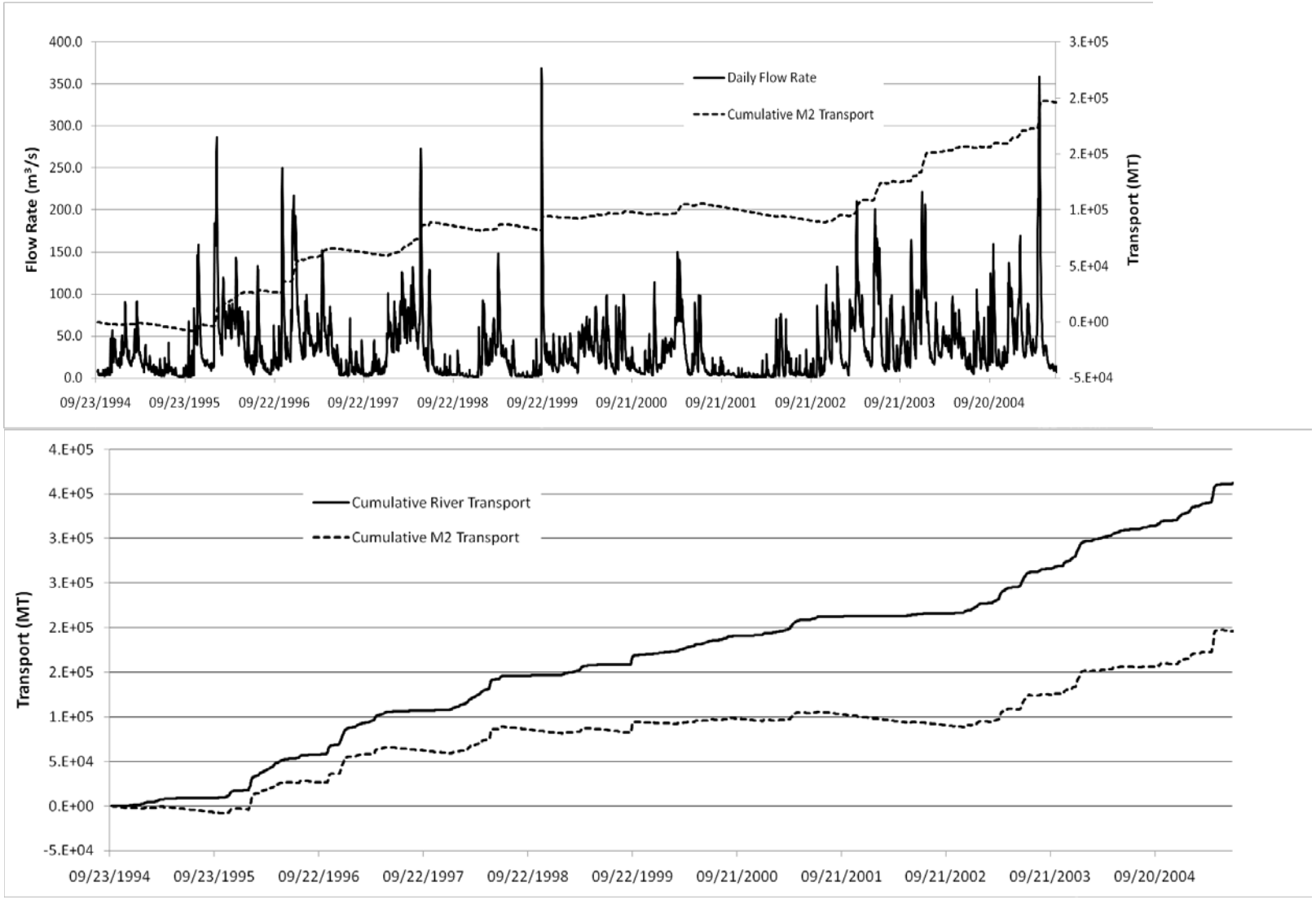

Figure 18. Flow rate and estimated cumulative transport near RM 3 (top) and cumulative river input from the Dundee Dam and estimated transport near RM 3 (bottom) from October 1994 through September 2005.

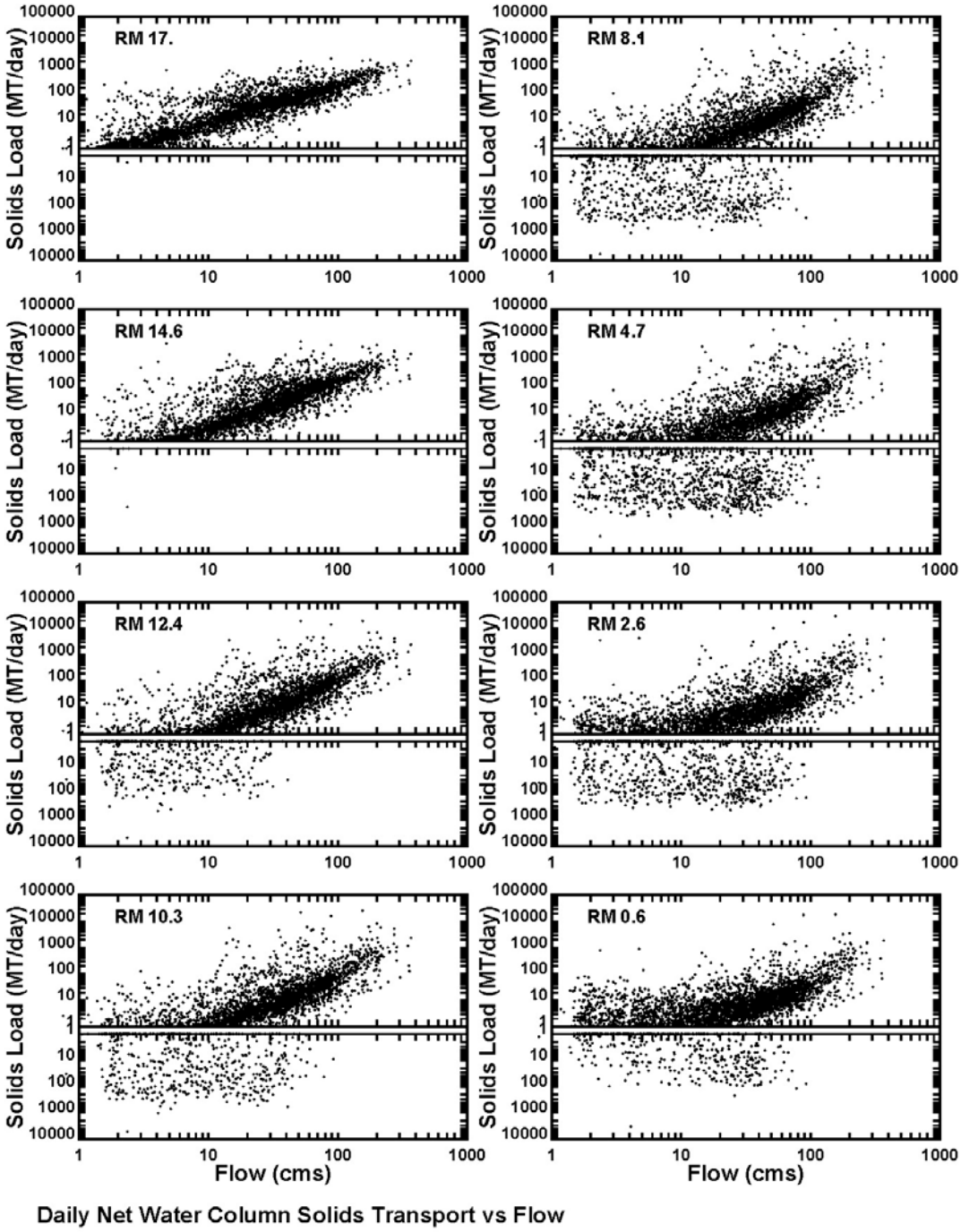

Figure 19. Daily water column sediment transport (negative is upstream) as a function of flow rate at 8 river mile stations in the Lower Passaic calculated from preliminary HQI hydrodynamics and sediment transport model.

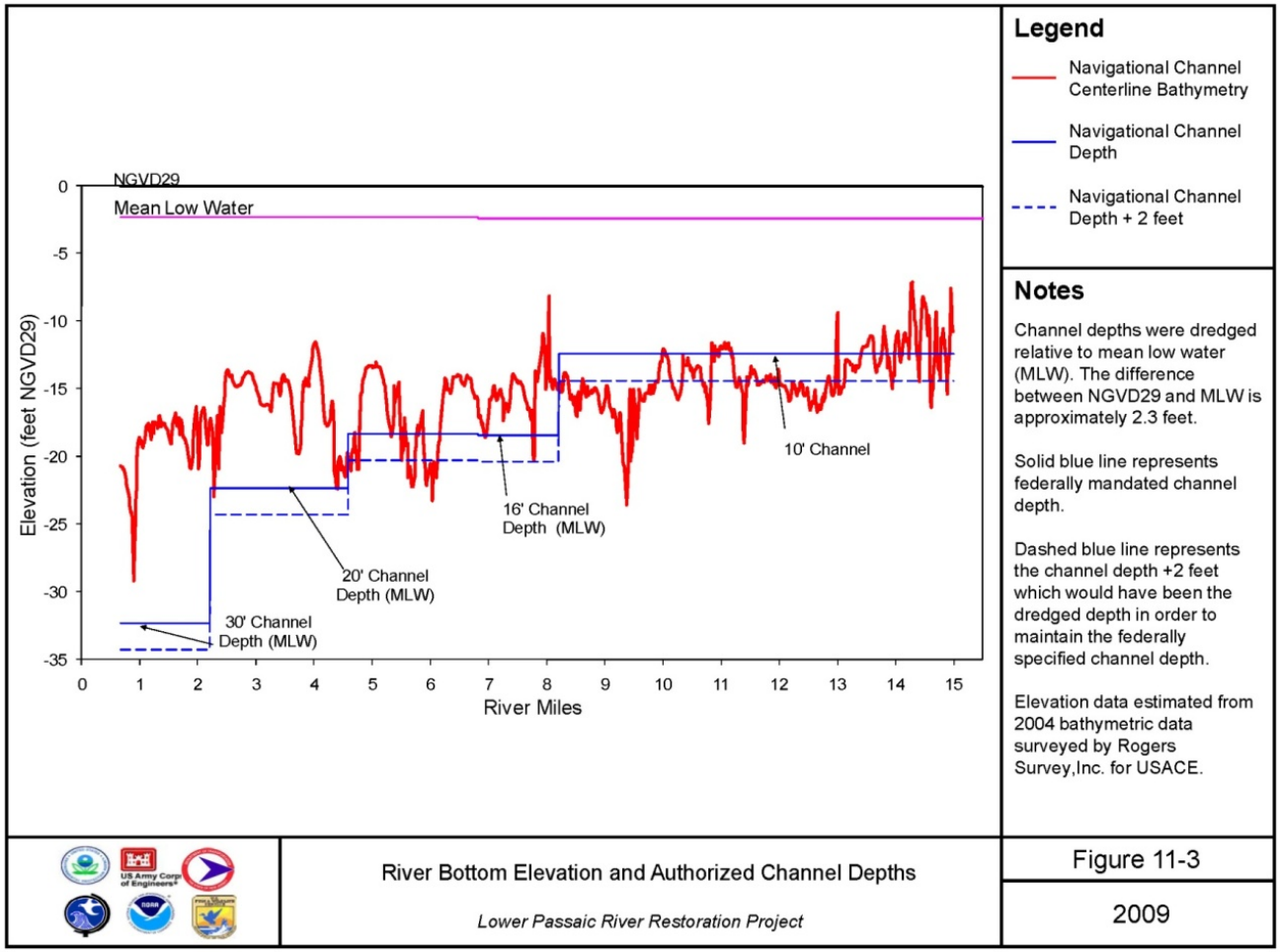

Figure 20. Depth of the river channel based on a 2004 bathymetric survey as well as the original dredged elevations as reported in USACE records.

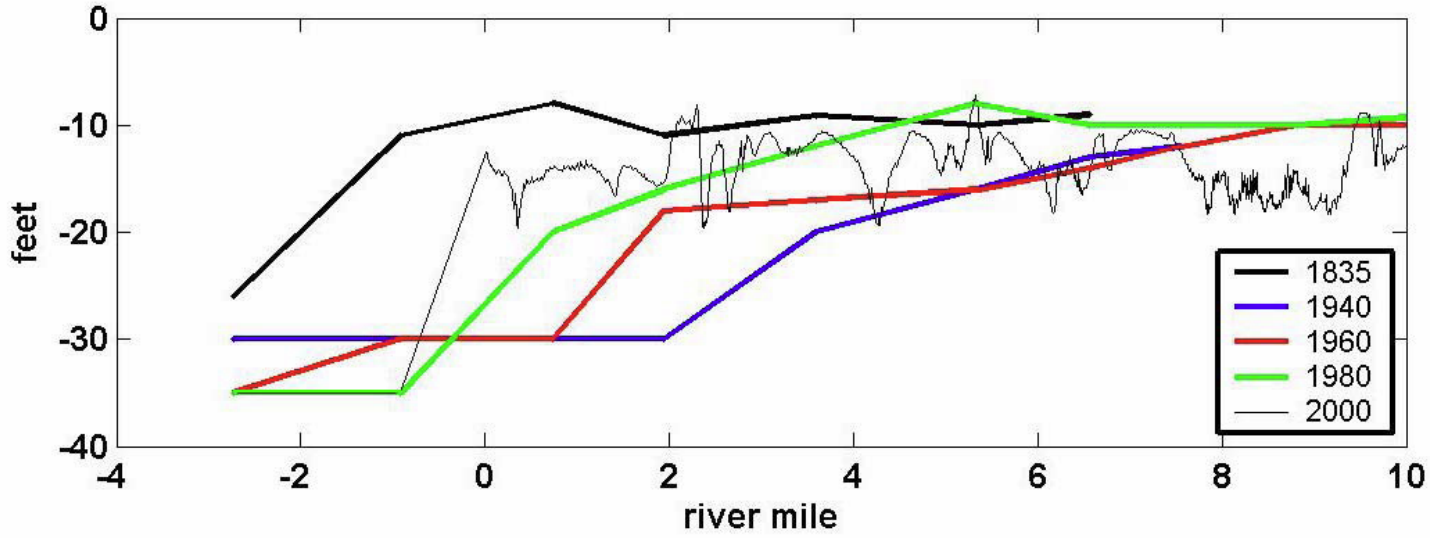

Figure 21. Estimated depths of the river channel from Chant et al. (2009).

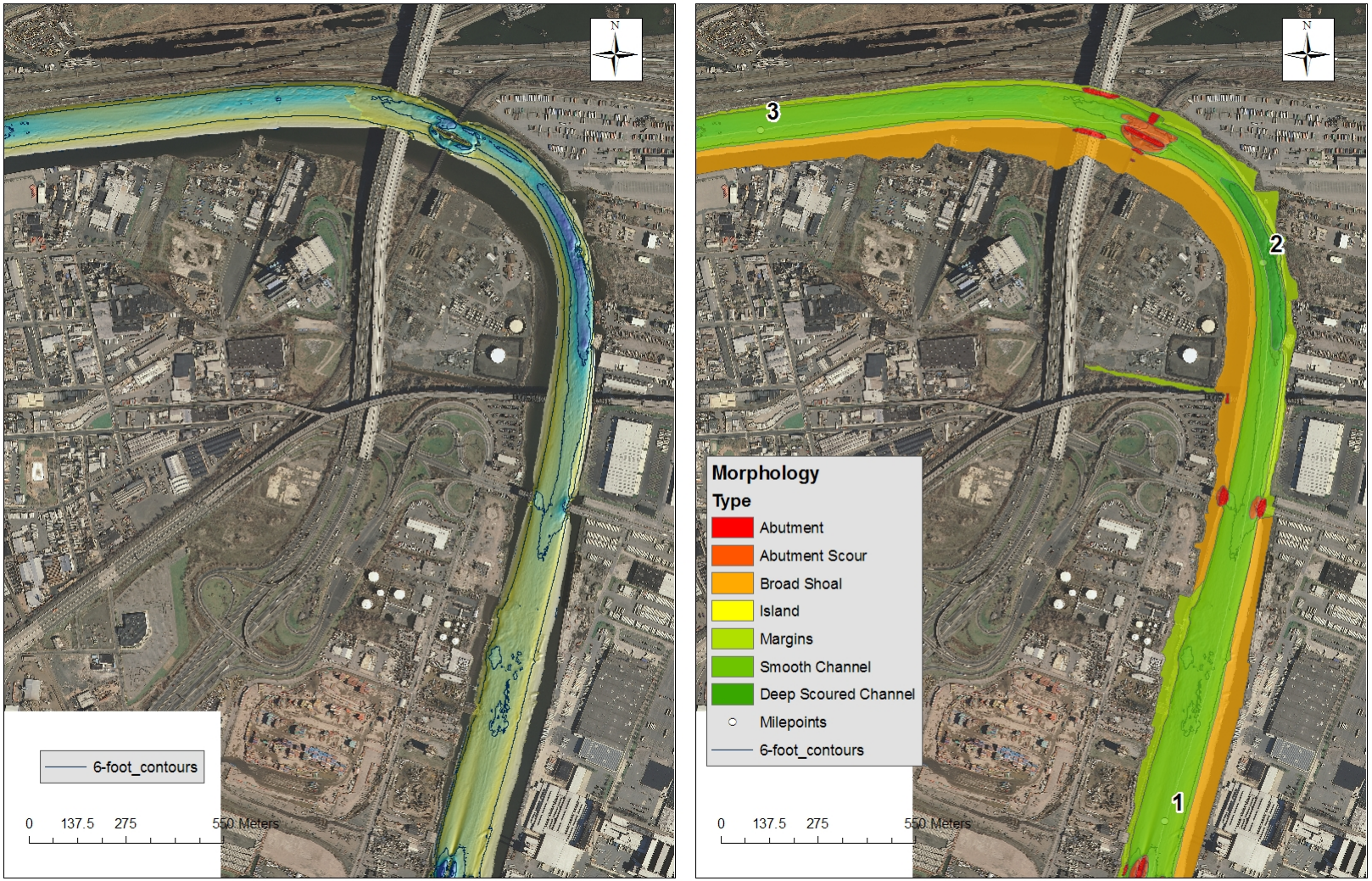

Figure 22. Shaded multibeam data and contours from the 2008 survey and an overlay of qualitatively identified morphologic regions near RM 2.

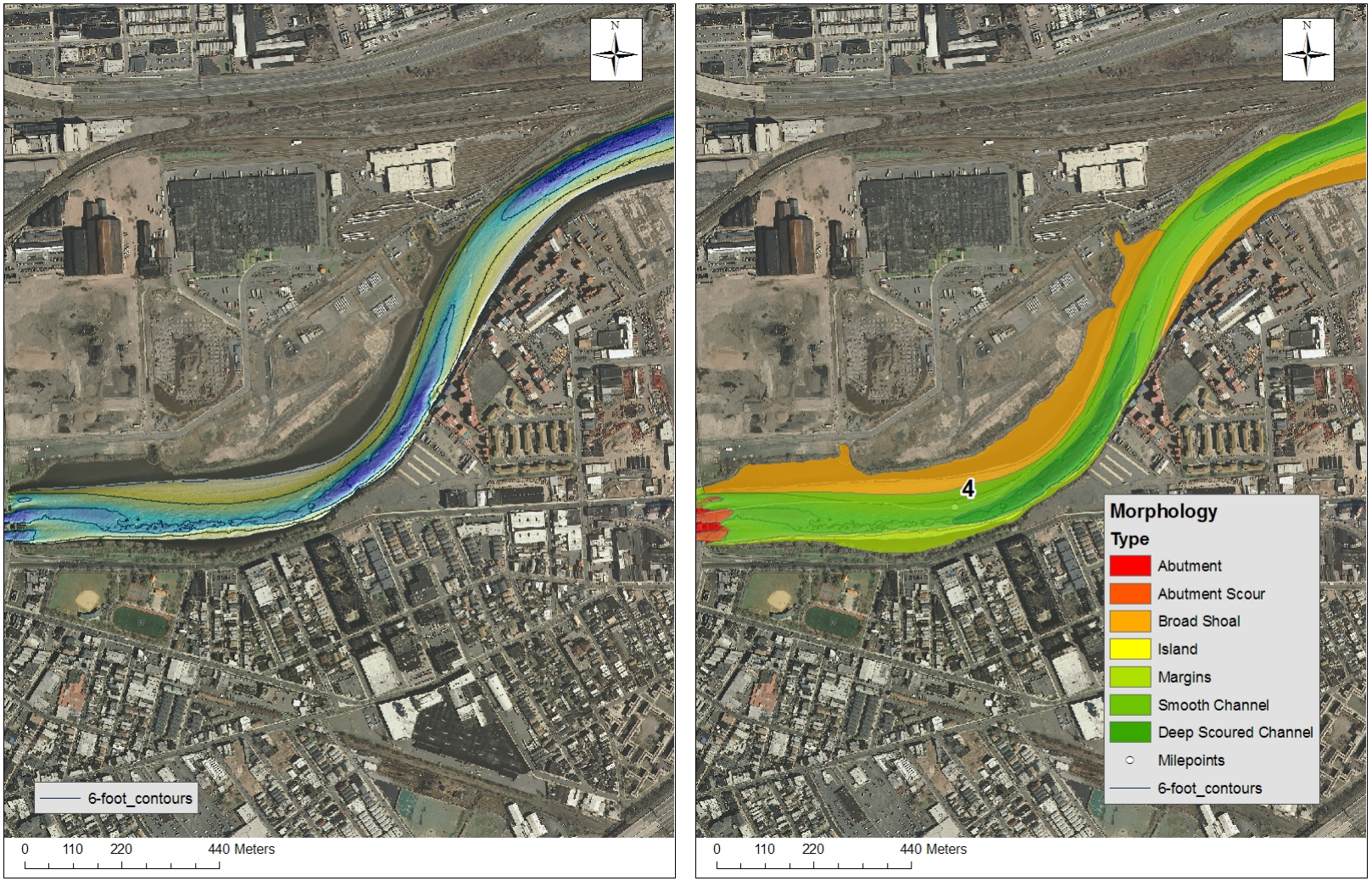

Figure 23. Shaded multibeam data and contours from the 2008 survey and an overlay of qualitatively identified morphologic regions near RM 4.

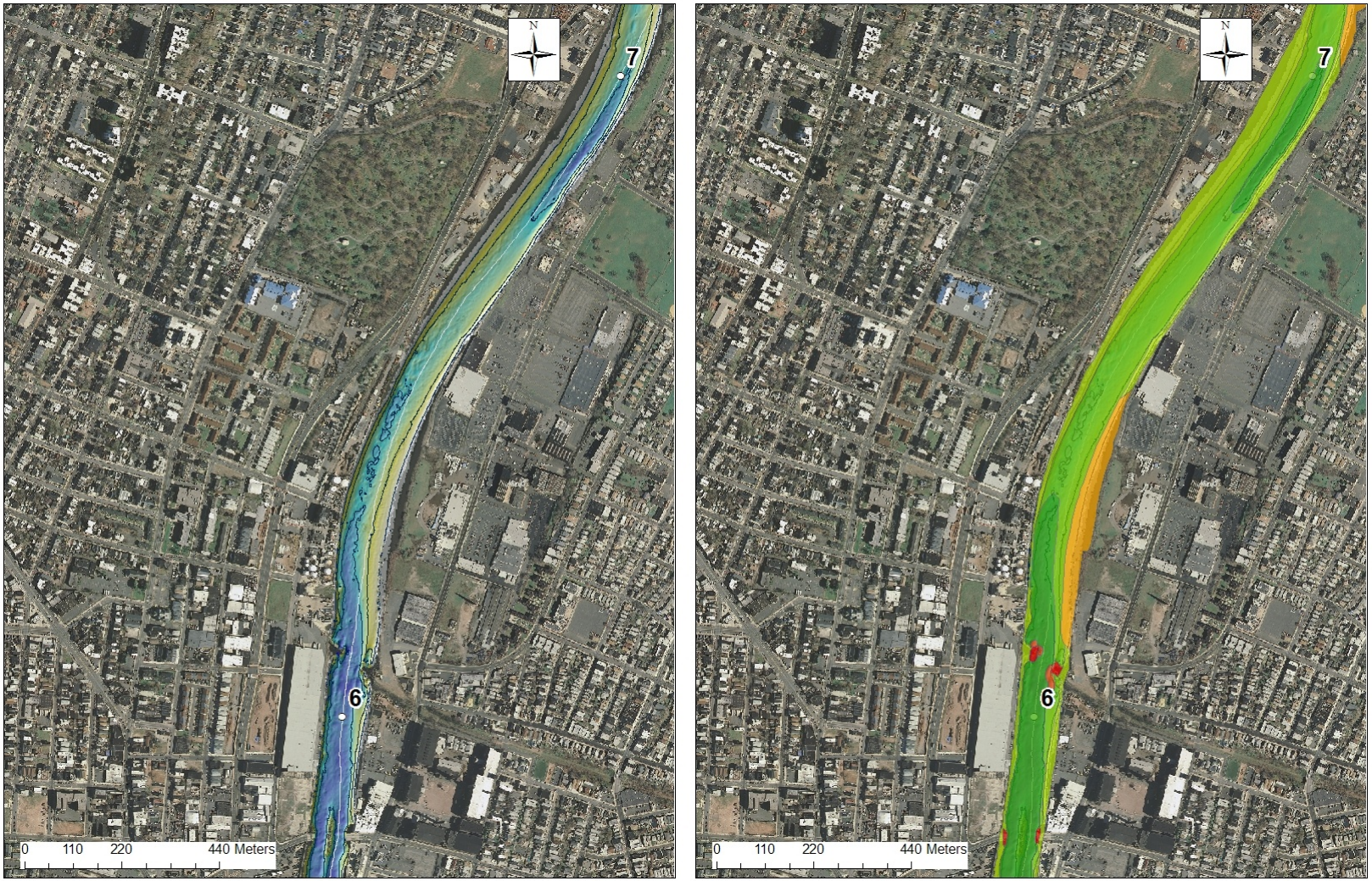

Figure 24. Shaded multibeam data and contours from the 2008 survey and an overlay of qualitatively identified morphologic regions near RM 6.

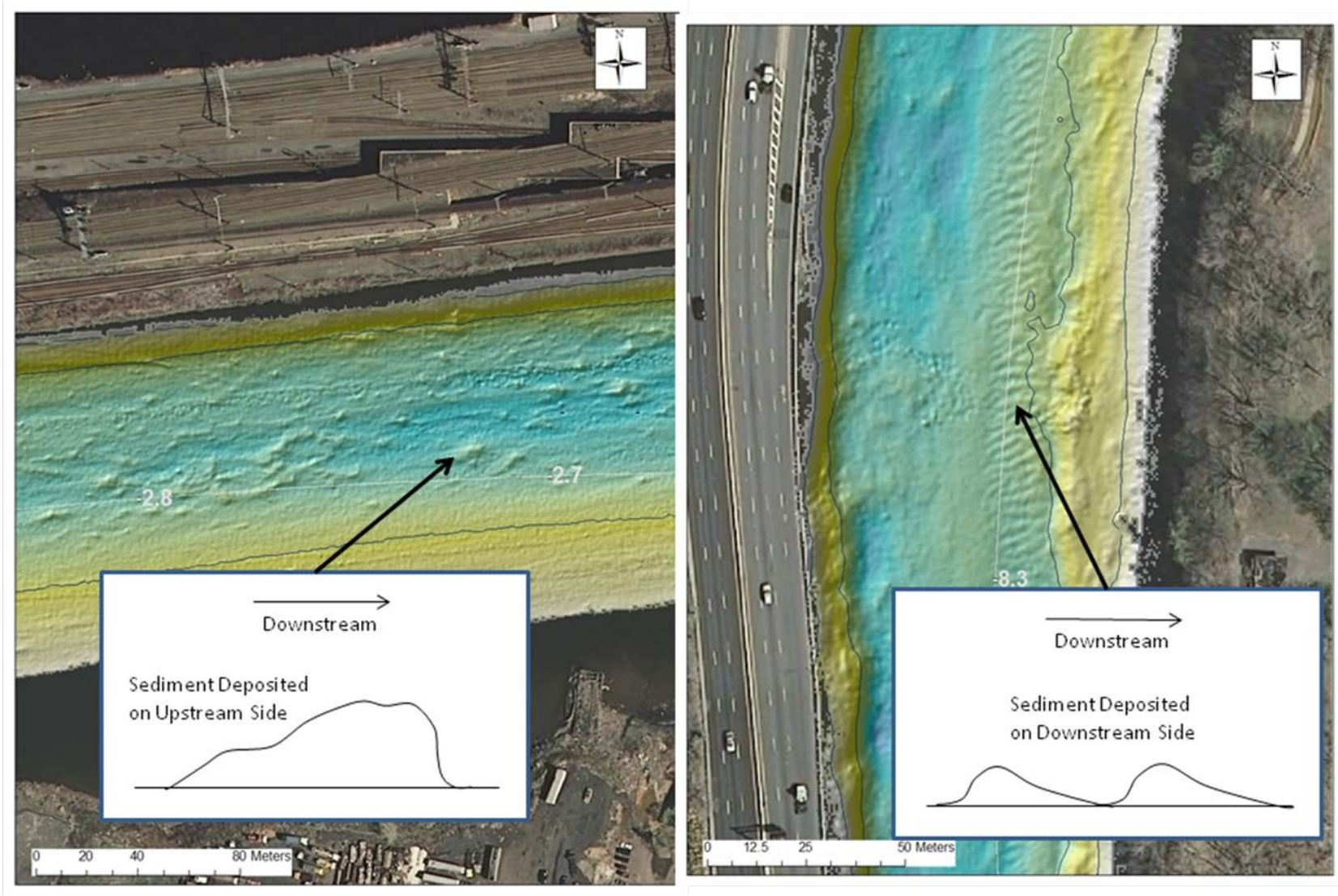

Figure 25. Shaded multibeam data from the 2008 survey highlighting bed features near RM 2.7 (left) and RM 8.3 (left).

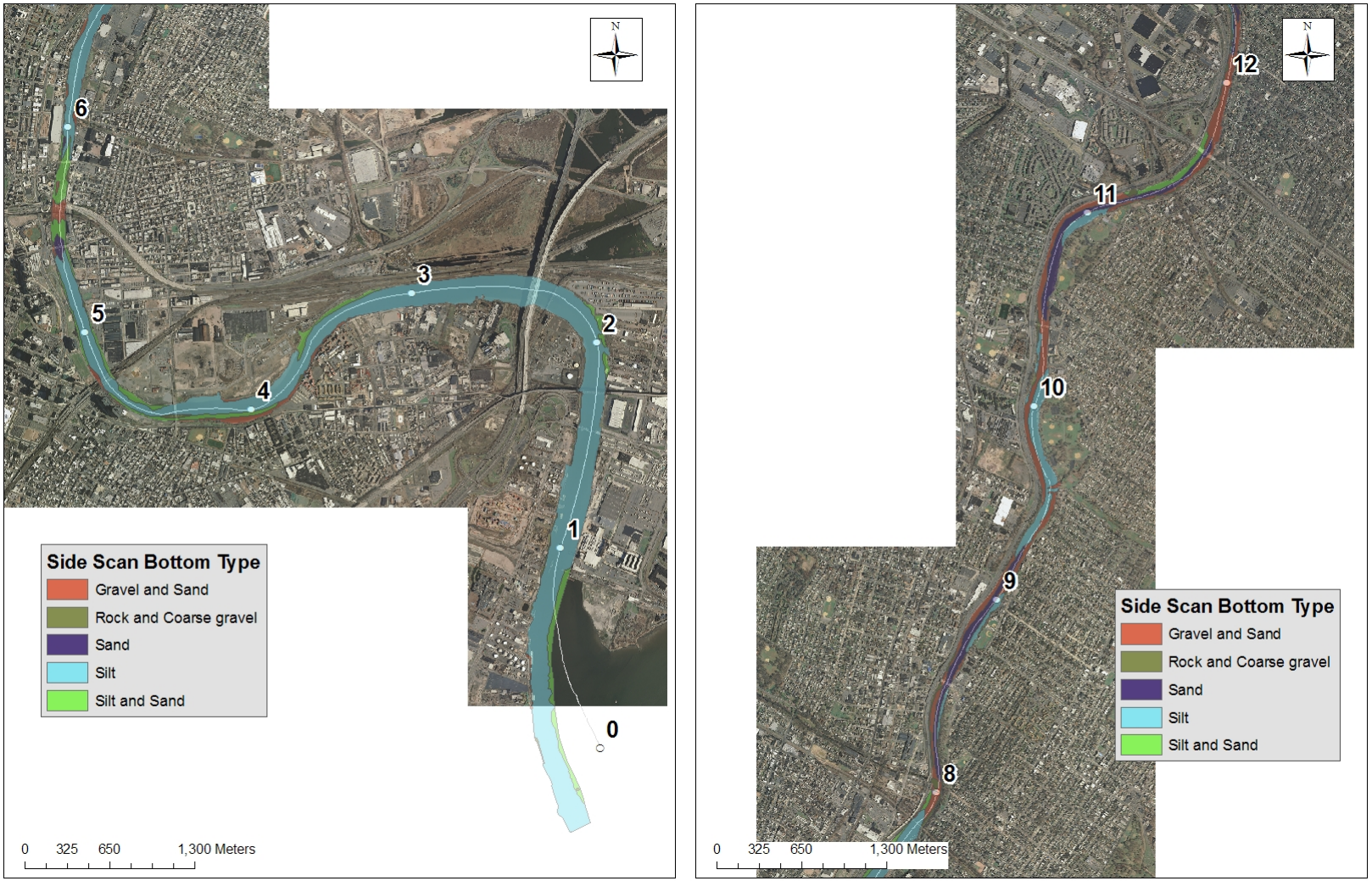

Figure 26. Side scan bottom texture identification from RM 0-6 and 8-12.

Figure 27. Side scan bottom texture identification from near RM 8

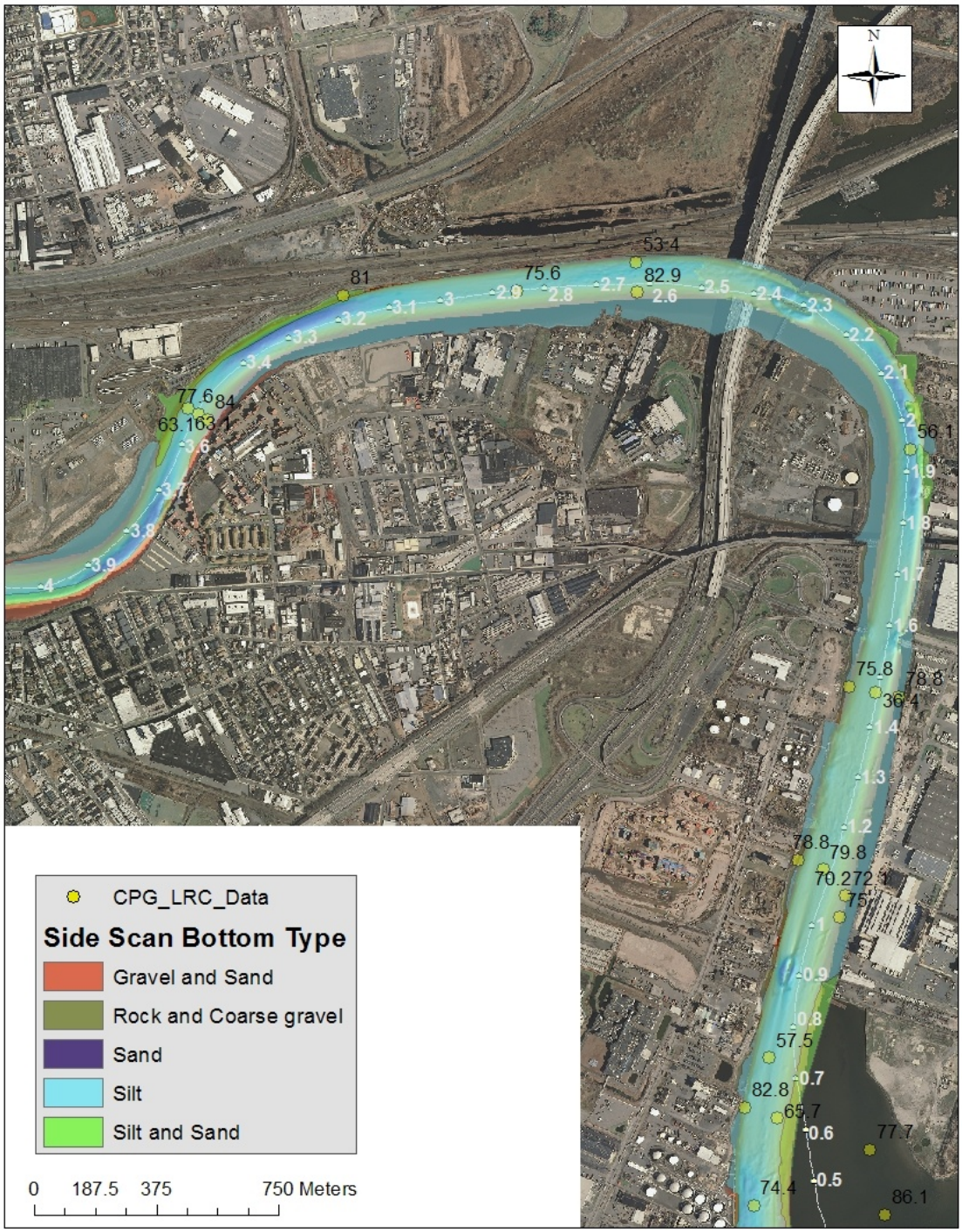

Figure 28. Side scan bottom texture identification and computed percent fines from the 2008 core data.

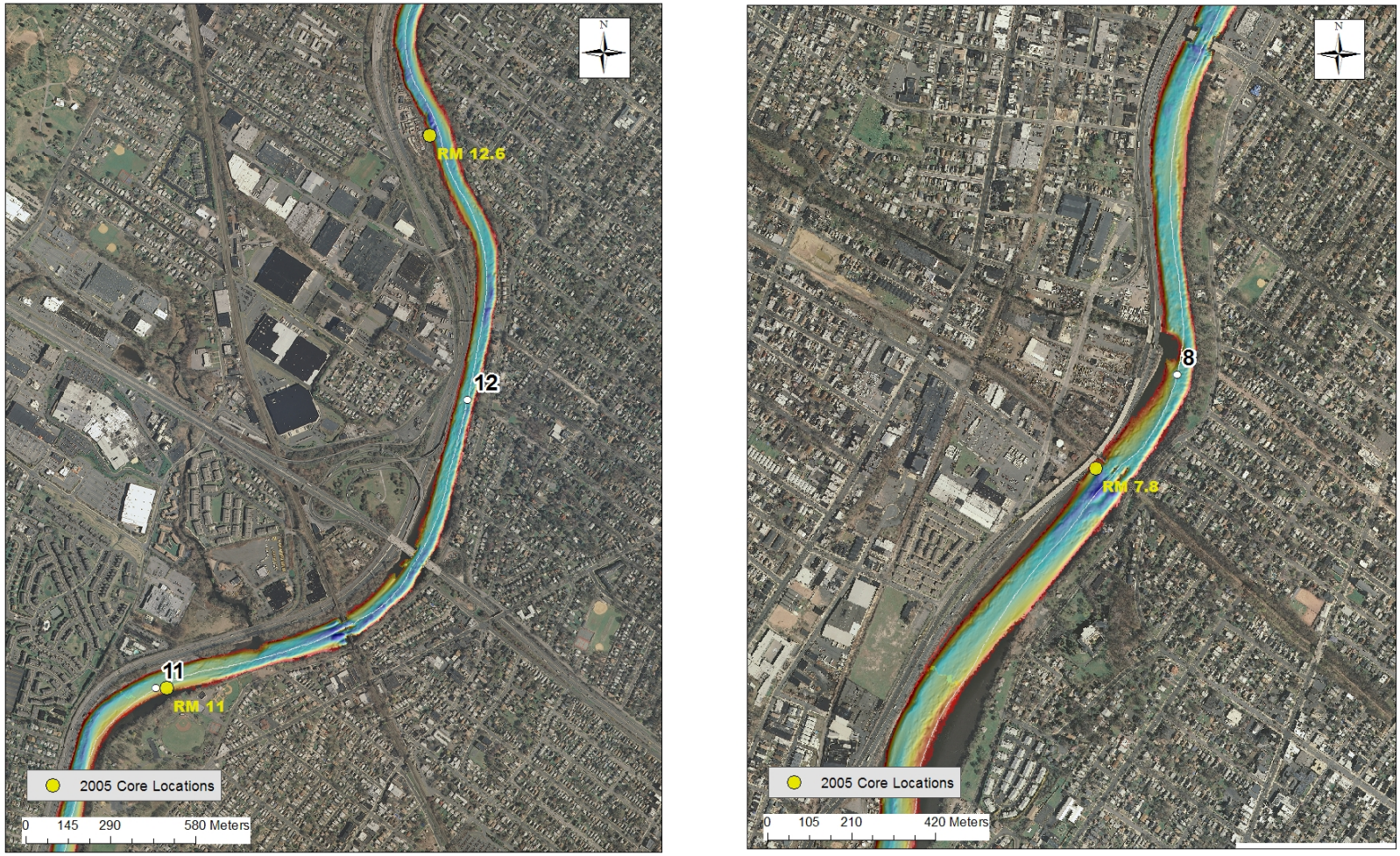

Figure 29. Locations of the three upper river 2005 CCSM cores.

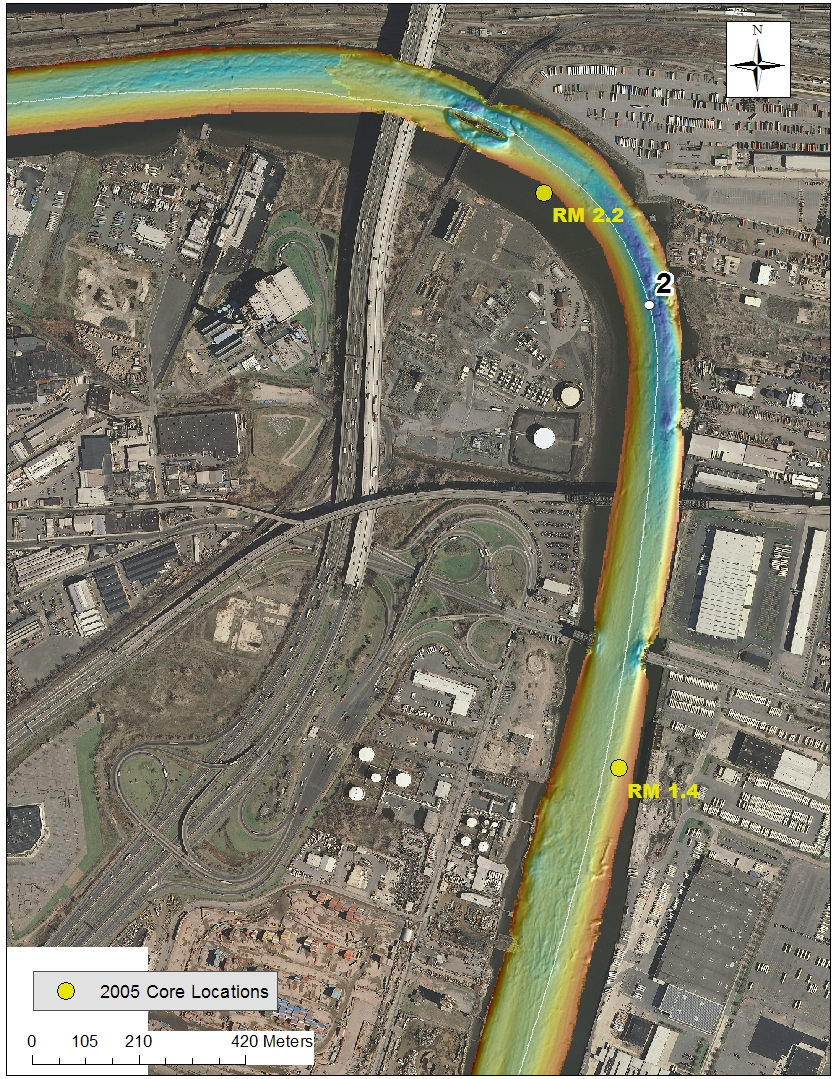

Figure 30. Locations of the two lower river 2005 CCSM cores.

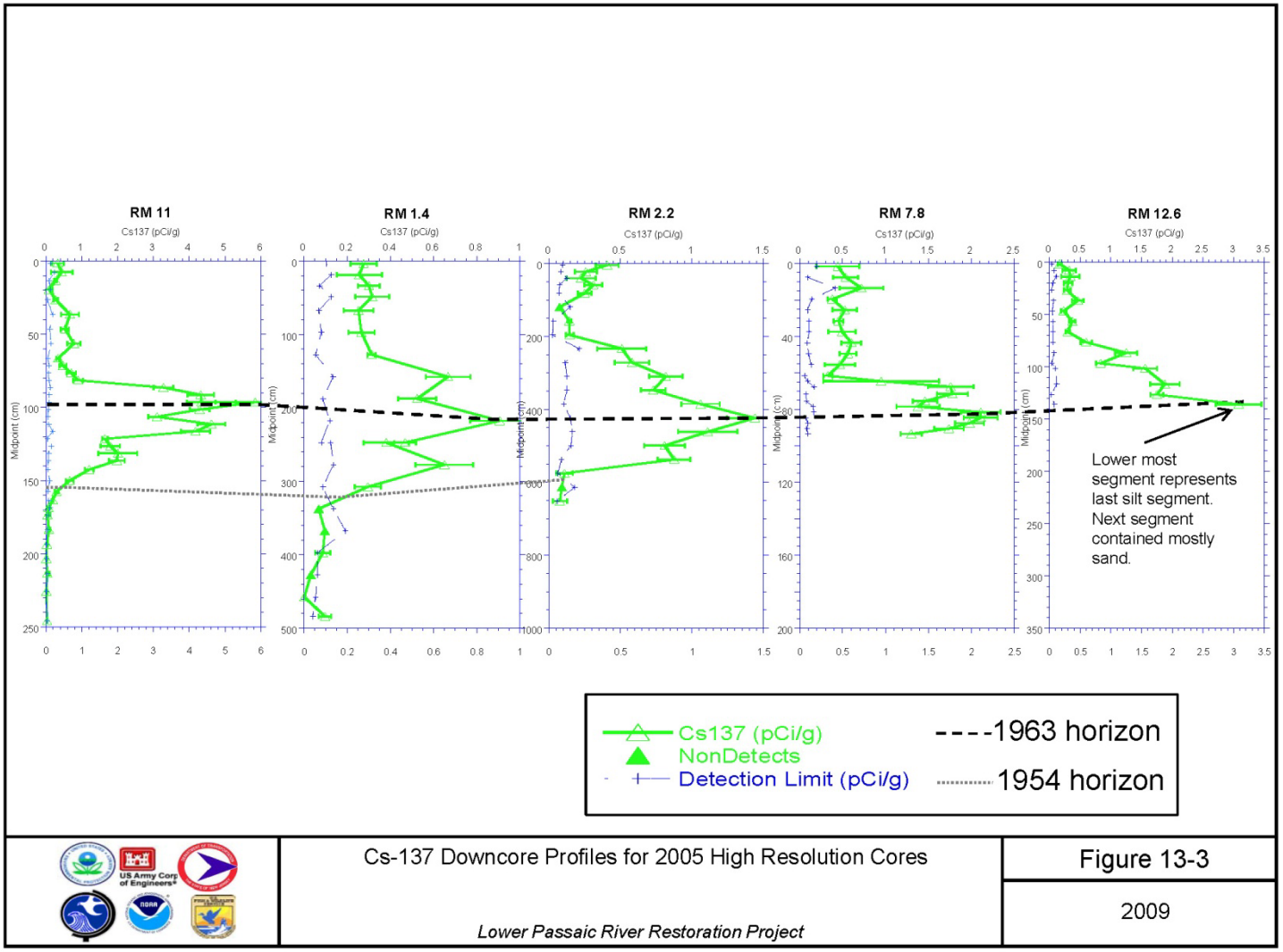

Figure 31. Profiles of Cs-137 for the 5 2005 CCSM cores with 1995 PCB profiles overlain.

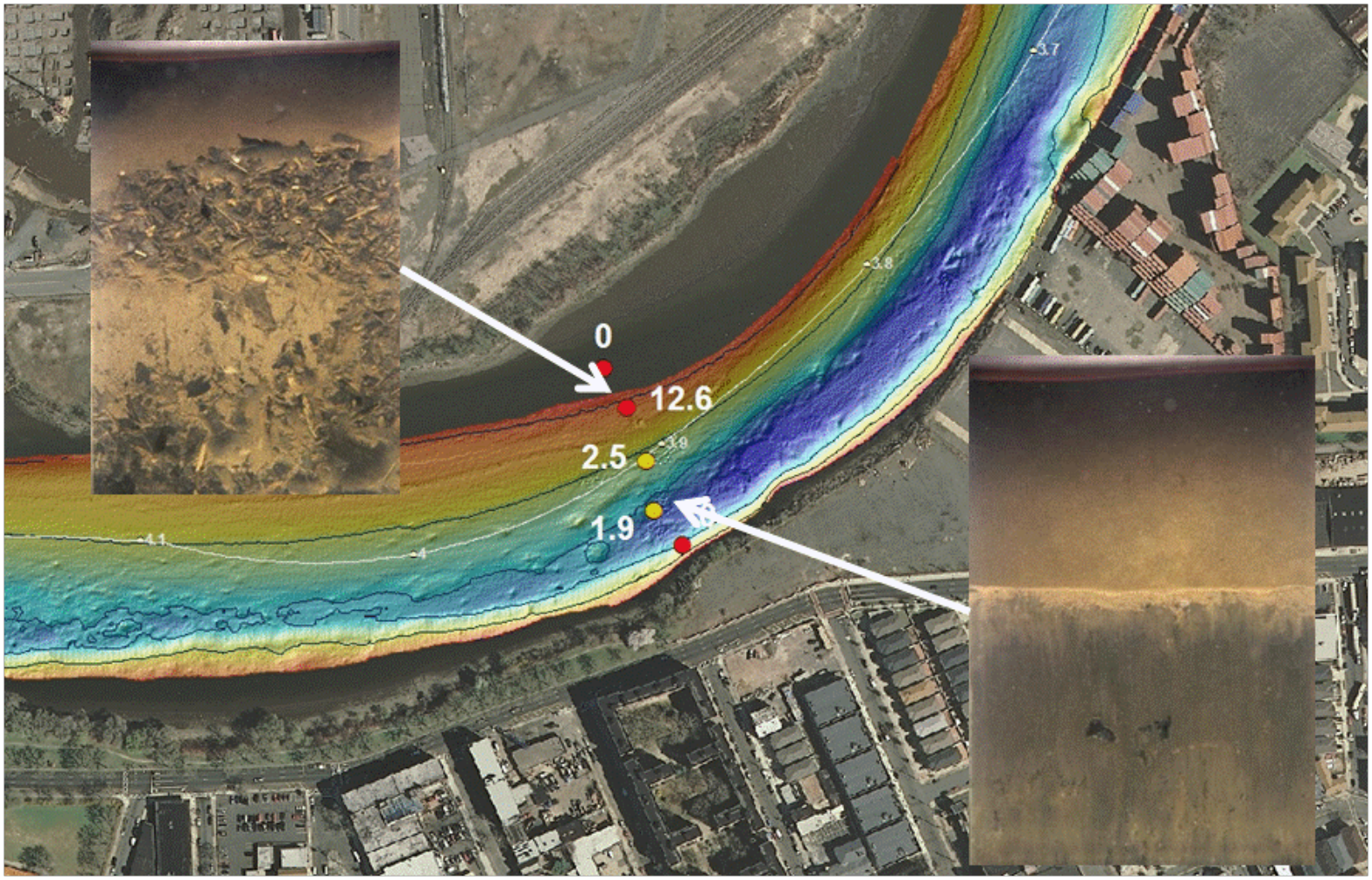

Figure 32. Shaded multibeam data from the 2008 survey and SPI camera deposition depths with photos at RM 3.9.

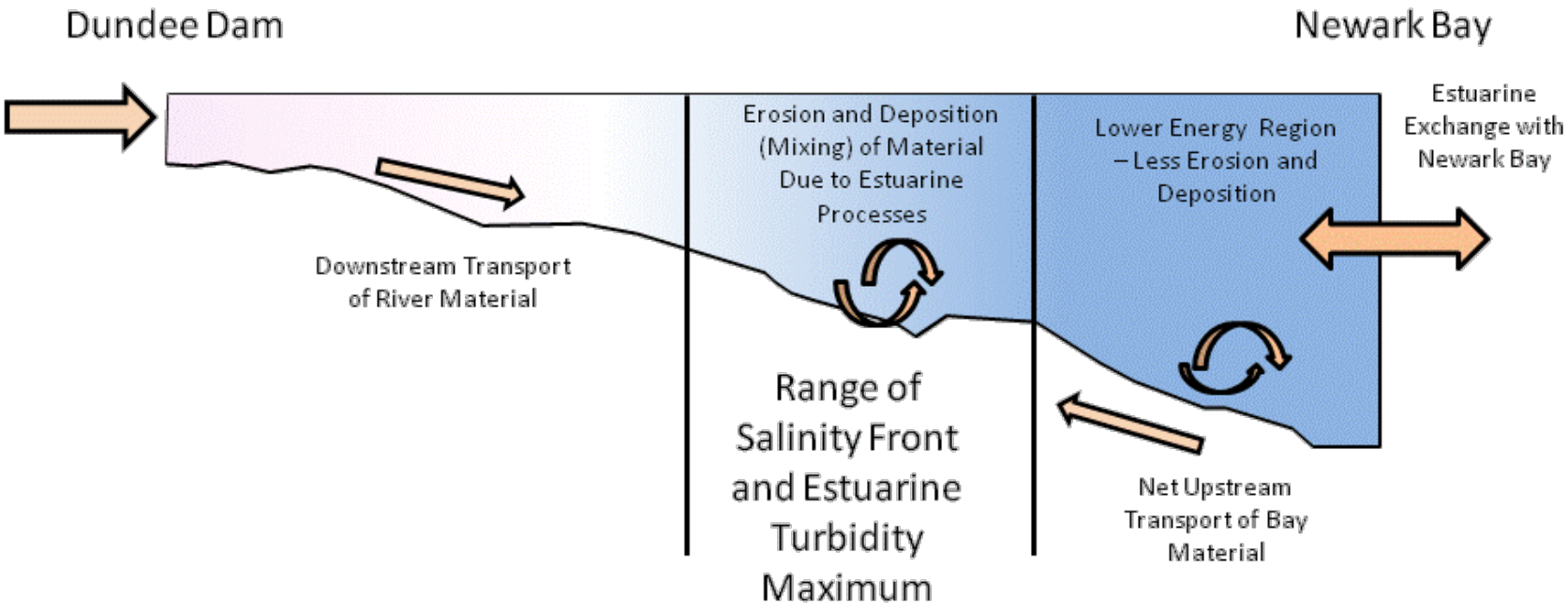

Figure 33.Conceptual diagram of key processes during low river flow conditions.

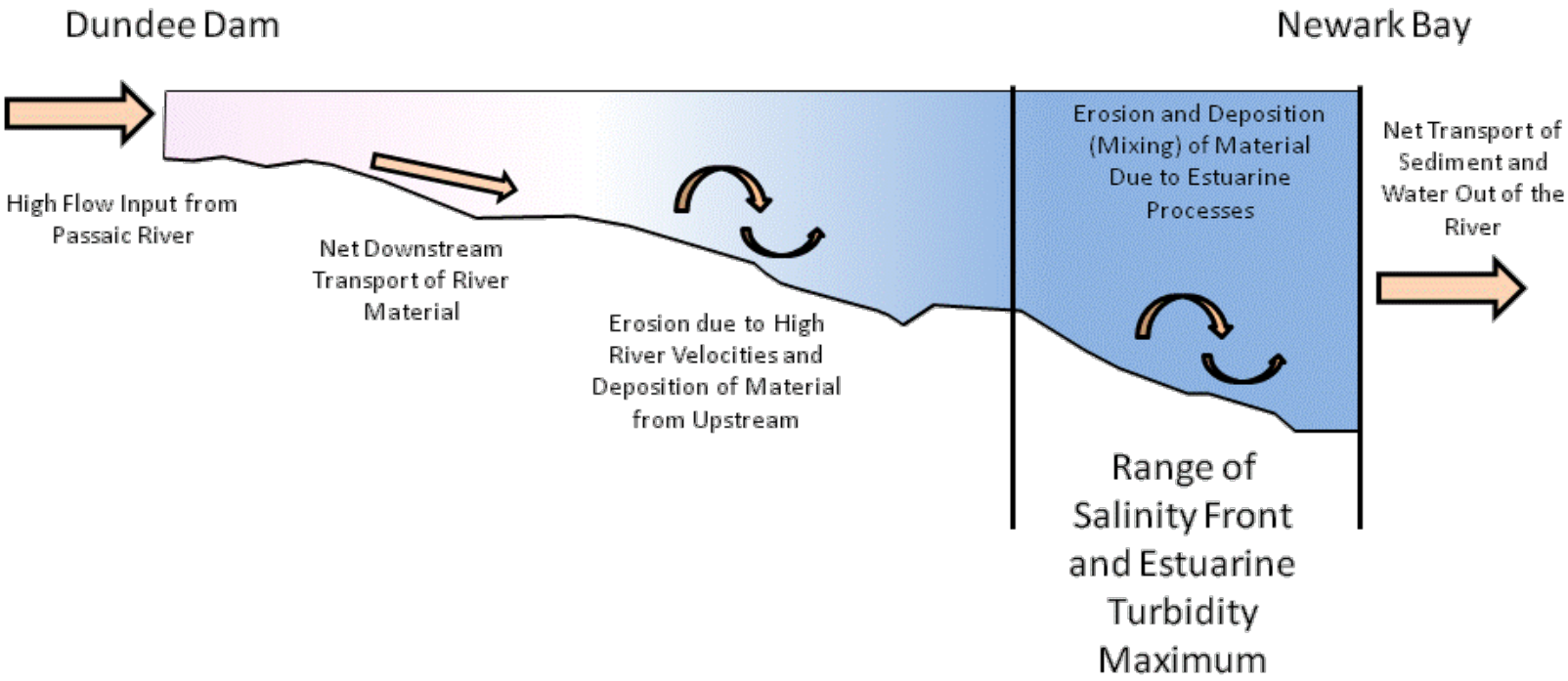

Figure 34. Conceptual diagram of key processes during high river flow conditions.